ARO 30066.1-CH-SB2

MOBILE ELECTRIC POWER

Final Report

D. P. Bloomfield, V. J. Bloomfield, P. D. Grosjean, J. W. Kelland
February 28, 1995

U.S. ARMY RESEARCH OFFICE
REFERENCE: P-30066-CH-SB2
Contract No.: DAAL03-92-C-0041
Completed on: December 31, 1994

Analytic Power Corp.
268 Summer Street
Boston, MA 02210
617-542-6352 (Voice)
617-695-3272 (FAX)

APPROVED FOR PUBLIC RELEASE;
DISTRIBUTION UNLIMITED

Acknowledgement

Analytic Power gratefully acknowledges the support of the Army Research Office as well as the Communications Electronics Command and the Army Research Lab for their support during this program. In particular, we would like to acknowledge the contributions of Dr. Richard Paur who offered timely assistance and advice during the course of the program. Many of the innovations that we successfully implemented were originally suggested by Dr. Paur.

MASTER COPY KEEP THIS COPY FOR REPRODUCTION PURPOSES

REPORT DOCUMENTATION PAGE

Form Approved
OMB No. 0704-0188

1. AGENCY USE ONLY (Leave blank)	2. REPORT DATE	3. REPORT TYPE AND DATES COVERED
	1995	Final Report

4. TITLE AND SUBTITLE

Mobile Electric Power

5. FUNDING NUMBERS

DAAL03-92-C-0041

6. AUTHOR(S)

D.P. Bloomfield, V.J. Bloomfield, P.D. Grosjean, J.W. Kelland

7. PERFORMING ORGANIZATION NAME(S) AND ADDRESS(ES)

Analytic Power Corp.
268 Summer Street
Boston, MA 02210

8. PERFORMING ORGANIZATION REPORT NUMBER

9. SPONSORING/MONITORING AGENCY NAME(S) AND ADDRESS(ES)

U. S. Army Research Office
P. O. Box 12211
Research Triangle Park, NC 27709-2211

10. SPONSORING/MONITORING AGENCY REPORT NUMBER

ARO 30066.1-CH-SBI

11. SUPPLEMENTARY NOTES

The view, opinions and/or findings contained in this report are those of the author(s) and should not be construed as an official Department of the Army position, policy, or decision, unless so designated by other documentation.

12a. DISTRIBUTION/AVAILABILITY STATEMENT

Approved for public release; distribution unlimited.

12b. DISTRIBUTION CODE

13. ABSTRACT *(Maximum 200 words)*

The objective of this program was to develop a mobile fuel cell power supply for use by soldiers. The Century Series of 100 through 500 watt fuel cell power supplies was developed.

The Century Series fuel cell power supplies are made up of a fuel cell stack, chemical hydride hydrogen supply, a fan and a controller. The FC-200, the 200 watt Century Series power supply, weighs 8.8 lb. and has a volume of 322 $in.^3$. The operating point is 0.7 volt/cell at 125 ASF; a power density of 22.7 watts/lb. or 0.62 watts/$in.^3$ and an energy density of 110 whr/lb. The prototype 750 whr hydrogen supply weighs 7 lbs. and has a volume of 193 $in.^3$. The fuel elements weigh 0.45 lb. and require 0.79 lbs. of water.

The FC-200 has powered a scooter requiring a starting current of three times the rated current of the stack. It has also powered a microclimate cooler.

14. SUBJECT TERMS

fuel cell, soldier power, power supply, hydrogen generator, chemical hydride fuel generator

15. NUMBER OF PAGES

43

16. PRICE CODE

17. SECURITY CLASSIFICATION OF REPORT	18. SECURITY CLASSIFICATION OF THIS PAGE	19. SECURITY CLASSIFICATION OF ABSTRACT	20. LIMITATION OF ABSTRACT
UNCLASSIFIED	UNCLASSIFIED	UNCLASSIFIED	UL

TABLE OF CONTENTS

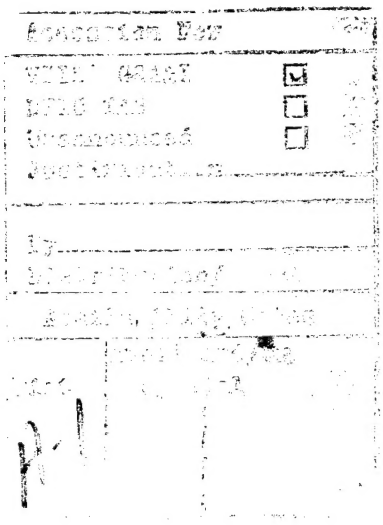

1. INTRODUCTION

The objective of this program was to develop a mobile fuel cell power supply for use by soldiers. The fuel cell power supply consists of a fuel cell stack, a chemical hydride hydrogen supply, a fan, and a controller.

When we began the program we were building 25 watt fuel cell stacks with a volume of 93 in3, a weight of 6.5 lb., and performance of 50 amps/ft2 (ASF) and 0.67 volts/cell. They ran on two reversible metal hydride filled cylinders weighing one pound each that lasted for a total of four hours.

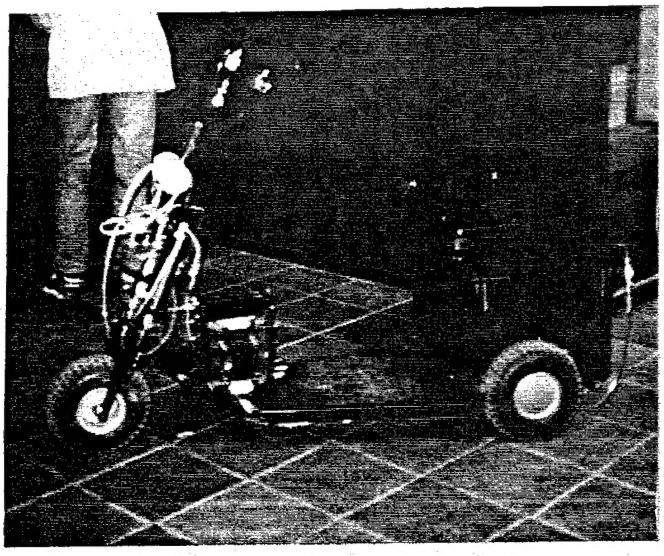

Scooter Powered by FC-200 and H_2 Generator

By the end of the program we had developed the Century Series of 100 through 500 watt power supplies. The FC-200, which is typical of these units, is a 200 watt power supply weighing 8.8 lb. and has a volume of 322 in^3. The operating point of the FC-200 is 0.7 volts/cell at 125 ASF. The fuel cell power density has been increased from 3.8 watts/lb. to 22.7 watts/lb. On a volumetric basis the power density has increased from 0.27 watts/in^3 to 0.62 watts/in^3. The FC-200 has powered a scooter requiring a starting current of three times the rated current of the stack. It has also powered a microclimate cooler.

We have increased the fuel cell stack energy density from 50 to 110 whr/lb. The hydrogen supply is a chemical hydride source that was developed in this program. The prototype 750 whr Fuel Pac hydrogen supply weighs 7 lb. and occupies 193 in^3. The Fuel Pac fuel elements weigh 0.45 lb. and the required water is 0.79 lb. This translates into 7 pounds for the first 750 whr and then 1.35 pounds (which includes 0.79 lb. of water) for each subsequent 750 whr of energy. As the mission time increases the energy density approaches the weight of the fuel or 1800 whr/lb. Reducing the fixed weight to fuel weight is a continuing objective.

This report describes the work performed in developing the Century Series of fuel cells and the chemical hydride hydrogen generators. The major findings are outlined in the conclusions and recommendations section. The results are fully described in the discussion section.

1.1 FC-200 (Type 4.1.5) Fuel Cell Stack

Type 4.1.5 Century Series Fuel Cells have been the high performance cell stack technology developed in this program. This stack technology addresses the twin problems of water and thermal management in small fuel cell stacks. These cell stacks have demonstrated:

- That ambient pressure air cooled fuel cells are limited by heat transfer.
- The effectiveness of forced convection cooling over natural convection.

- The importance of controlling capillary forces in the flow fields through hydrophylic treatment of materials and incorporating wicks to transfer water from the cathode to the cooler flow fields.
- Current densities 3 to 5 time larger than their predecessors at a given cell voltage

A number of advances were made in the electrochemical components of the cell stack. These include successfully printing catalyst layers on very thin Nafion films and making the cells tolerant to "gels" in the membrane which have caused crossover and shorts in the past.

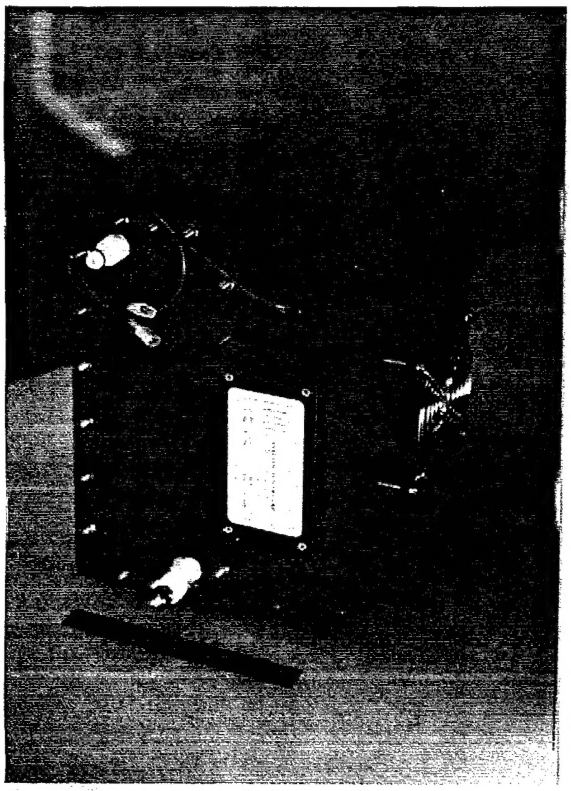

FC-200 Century Series Fuel Cell Stack

1.2 FC-150 (Type 4.2) Fuel Cell Stack

While the Century Series Type 4.1.5 cell stacks proved to be the high performance stacks developed in this program, the FC-150 has been the principal learning tool. The FC-150 is a small format (2.5" in. x 2.5") 39-cell fuel cell stack. A design objective of the FC-150 was to build a 28 volt fuel cell stack. Compared to the Century Series cell stacks, the FC-150 has a reduced cell area and an increased number of cells. We also reduced the thickness of the air cooler and cathode plates in an effort to shorten the stack. The long, narrow FC-150 required using two propeller type fans. We initially used a "pusher" flow for the fan but the "shadow" under the fan hub and the decrease in air flow to the end cells limited performance of the FC-150 to the level of a natural convection stack. Its performance level never rose over 40-50 ASF at 0.7 volts/cell

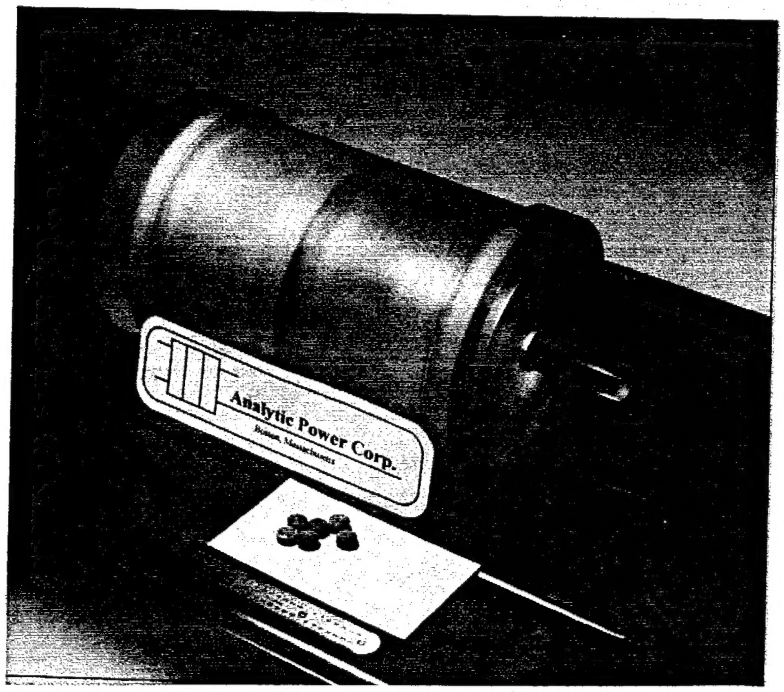

Experimental Chemical Hydride H_2 Generator

1.3 Fuel Pac

We investigated several types of fuel reactors and a number of chemical hydride chemistries. A program objective was development of a position independent reactor that can utilize the very high energy density of sodium borohydride. This is the material of choice since it is used

on a large scale by the paper making, pharmaceutical and petroleum industries. It is also safe and easy to handle.

Packaging the borohydride and controlling the reaction were successfully developed in this program. The fuel cell powered scooter was fueled by a binary liquid, chemical hydride, hydrogen source.

2. CONCLUSIONS & RECOMMENDATIONS

2.1 Fuel Cell Stacks

Fuel cell performance is defined as the current density a cell reaches at a given cell voltage. In most applications the optimum weight volume and cost of PEM fuel cells is obtained at 0.7 volts per cell. High fuel cell performance means high current density at a design voltage such as 0.7 volts per cell. In this program we demonstrated reliable performance at 150 ASF and 0.7 volts per cell.

2.1.1 Thermal Management

For reliable high performance, air cooled fuel cell stacks must be forced convection cooled and the cooling and cathode channels must be separate. Work on the Type 4.1.3 and Type 4.1.5 cell stacks showed that air cooled PEM fuel cell stacks are heat transfer limited.

In single cell tests we have shown that the 2.5" x 2.5" FC-150 cells can easily operate at 120°F and 300 to 500 ASF at ambient pressure. At high pressure and temperature the same cells have demonstrated 0.72 volts per cell at 1000 amp/ft^2. The limiting current density of the cells on hydrogen and oxygen is in excess of 6,000 ASF. The stack cannot handle waste heat fluxes of greater than about 80 watts per square foot ($WSF_{thermal}$). This limits the maximum continuous current density.

2.1.2 Air Flow

In the FC-150, the low cooling air flow increased cell temperature resulting in membrane water loss which caused membrane resistance to rise. Experiments and analyses of pressure drop versus flow show the ratio of cooling to reactant air was only about 2:1. Too much air passing through the reactant channels cause the membranes to dry out and cross over; especially in the hot parts of the stack. In this report we will show the required relationship between cooling and reactant air flow is usually in excess of 10:1 for optimum cell performance. Detailed modeling and experiments conducted during this program point to the requirement for adequate flow field design. Coupling between the flow field and the fan is an important consideration in this design process.

2.1.2.1 Thermal Instability

A stack with inadequate air flow is thermally unstable. By this we mean that performance declines and the stack drops load until its output power is close to zero. In our early natural convection cooled Type 4.1.3fuel cell stacks this was the most common cause of failure.

2.1.2.2 Fans & Blowers

Achieving a high air flow in a thin cooler plate is a challenge. It is possible to increase air flow using a blower rather than a fan. Most low flow blowers develop up to a 0.8 inch of water pressure rise. Blowers do not integrate well with cell stacks due to the shape of the blower outlet.

2.1.2.3 Ports & Manifolds

Evenly porting the reactant air to the cells remains a difficult problem. A flow split controller is required to ensure that most of the air is ported through the coolers rather than the cathodes.

Another finding in air manifold design is that the "no-flow shadow" under a propeller fan hub is significant. EG&G's Rotron Division indicated that the pusher fan should be no closer than 1.5 fan diameters from the surface of the stack. This results in a very high manifold. Using the fans in an "exhauster" configuration permits a lower manifold and uses the cooler channels as a flow straightener. Transaxial flow fans also offer a low profile manifold but at a much lower pressure rise. Coupling the fan, the manifold, and the cell stack has proven to be an important part of the design process.

2.1.2.4 Roll Fins vs. Carbon Flow Fields

A modification of the design developed in the program was the use of "roll fins" which are a form of textured sheet metal. The use of these fins was suggested by the Army. The lanced and offset pattern roll fins preserve the compact package of the FC-150 yet they increase the cooler channel cross-sectional flow area.

Carbon cooler flow fields have an electrical resistivity of over 50 times that of stainless steel. Because the principal resistance in fuel cell stacks is contact resistance, the intrinsic resistance of carbon may not be too important. Titanium nitride would have an even more conductive surface than stainless steel. The advantage of stainless steel over titanium is that stainless steel does not require nitriding. Experiments are presently underway to determine the dimensional stability of titanium roll fins during the nitriding process. The high temperature used in nitriding often warps and expands the metal.

2.1.3 Structures

Cell planarity affects stack electrical resistance in the fully compressed stack. Achieving a planar unit cell is no mean feat since the compliance of the cell elements range from soft plastics to carbon papers having the structural properties of ceramics. Many of the cell elements have highly non-linear compression characteristics. The grooved carbon flow fields which we extended through the cell frame to form port bridges and had low shear strength. These carbon paper port bridges were replaced by expensive plastic port bridges. With the lanced offset roll fins the structure becomes stronger and the plastic port bridges can be eliminated.

2.1.4 Weight

Stack weight is related to cell pitch, the number of cells per inch of stack length. Using roll fins, the reduction in stack weight comes not from the roll fins themselves but from the increase in cell pitch due to thinner flow fields. The plastic hydrogen manifolds are thinner and the port bridges are eliminated which dramatically affects stack length.

Using the roll fin matrix we can eliminate the carbon flow fields and port bridges in the cooler. This drops the stack weight by 0.62 lb. We add just over 1 pound back in stainless steel fins. So the weight penalty is 0.4 lb. A titanium fin requires a slightly thicker metal (0.005 in.) for structural reasons but does not greatly affect any other factor. Because it has half the density of stainless steel it yields a slightly lower weight penalty of 0.34 lb. During operation the porous carbon flow fields can fill up with an extra pound of water.

Additional weight reduction can be achieved by replacing the carbon cathode flow field with a plate/fin matrix. This reduces the thickness of this piece since the flow requirements are $1/20^{th}$ that of the coolers. Roll fins as cathode flow fields reduce stack length.

2.1.5 Water Management

The fuel cell stacks developed in this program operate on dry hydrogen and ambient air. The use of thin membranes facilitates this operation. Hydrophilic carbon flow fields developed under this program also aid in water management. The air flow through the cell stack is designed to remove water vapor at all operating conditions. The flow fields and auxiliary wicks ensure water management during upset conditions. The cathode wicks are connected to the cooler flow fields to take advantage of the larger cooler air flow rate for evaporation. Since the coolers are hydrophilic the water is distributed across the entire surface of the cooler. This permits the use of all the cooling channels for evaporation.

2.1.6 Cost Analysis

In terms of cost, the roll fin matrix has an advantage over the standard hardware. In the FC-150, eliminating 78 machined ULTEM port bridges at $11.75 a piece saves almost $1000. Machining is required because of the thin backbone connecting each channel. The carbon flow field materials and labor amounts to another $200 savings. The material cost of stainless steel is only $12.85 per stack. The cost of forming it into a roll fin matrix is significant in small quantities, $19.86 per piece. This translates to a stack cost savings of $330. However, in larger quantities the price drops significantly yielding a reduction in stack cost of about $1,070 for the coolers alone. Titanium is considerably more expensive per pound than stainless steel but the material cost is a small portion of the total.

A conclusion of this program is that carbon paper is expensive in large quantities and very expensive in small quantities. It has a low conductivity and a low strength. Its use virtually precludes a low cost commercial fuel cell stack.

2.2 Chemical Hydride Fuel Generators

2.2.1 Timing and Control

The reactor consists of sodium borohydride, cobalt chloride pellets and a pressurized water supply. The water is admitted to the reactor through a solenoid control valve which is controlled by a reactor pressure signal and a timer. The timer protects against adding too much water during any time period thus compensating for variations in reaction rates due to reactant depletion. The generated hydrogen gas is slightly pressurized and regulated to the anode where the pressure is no more than about 5 psi. Slight pressurization of the reactor makes it possible to control the system.

The maximum pressure in the reactor is dictated by the control system accuracy. The more accurately we control the inlet water the smaller the required reactor volume.

2.2.2 Reactor Materials

Reactor materials are important in reducing reactor weight. In this program, the borohydride weight is about 6.5% of the reactor weight. The water is a little more than 10% of the reactor weight. The unreactive (hardware) weight fraction of the reactor is inversely proportional to the energy capacity required by the reactor.

2.2.3 Fuel Form

Fuel in the form of commercially available pellets or specially bonded plastic pucks was evaluated. We also investigated binary liquid reactors. While the binary liquid reactors are easily controllable and have moderate energy densities, they were rejected because the hydride liquid freezes at 50°F and lower.

Encapsulating a pellet form of the sodium borohydride in a gas permeable reactor appears to be the optimum solution to chemical hydride reactors. Water distribution to and throughout pucks led to their rejection. Hydrate formation is a problem in obtaining the maximum yield from borohydride reactors. The reaction rate is controlled by temperature, pH, and the presence of catalysts.

2.2.4 Energy Density

The energy density of the Fuel Pac is a strong function of the mission energy requirements. The systems we developed can control the chemical hydride operation but non-reactive weight is a significant portion of the hydrogen generator weight. The major source of non-reactive weight is the controls and the shell that houses the reactor and water. Future development should concentrate on minimizing the non-reactive portion of Fuel Pac weight. This extends the competitive advantage of fuel cells into the advanced battery realm.

3. DISCUSSION

3.1 Cell Technology

3.1.1 Performance

3.1.1.1 Single Cell Performance

Single cell performance continues to improve. At high pressure, cell voltages of 0.7 and 1000 ASF are routinely obtained. At low pressure, and 0.7 volts, we have obtained up to 500 ASF on advanced cell membranes as seen in Figure 1. The catalysis procedure Analytic Power jointly developed with DuPont has remained unchanged. Membrane thickness reduction and quality improvements (freedom from gels) have raised performance levels. Fuel cell heat transfer prevents us from taking advantage these high performance levels.

3.1.1.2 Fuel Cell Stack Performance

While single cell performance levels show that current densities of 500 ASF are achievable at reasonable cell voltages, air cooling limits performance to about 0.7 volts per cell at 150 ASF.

This corresponds to a heat flux of about 80 watts/ft^2 (280 BTU/ft^2). Liquid or two phase cooling will permit very high current densities at low pressure. In the following sections we will discuss the performance milestones of fuel cell stacks built in this program.

3.1.1.2.1 Five Cell Sub-Stack (Stack #2)

The development of Stack #2, a five cell substack using natural convection and designated as Type 4.1.3, resolved the problems of planar cell design and we started to explore the effects of heat and water management on fuel cell stack performance. This stack test was the first in a series which eventually led to forced convection over natural convection cooling. Stack #2 employed natural convection.

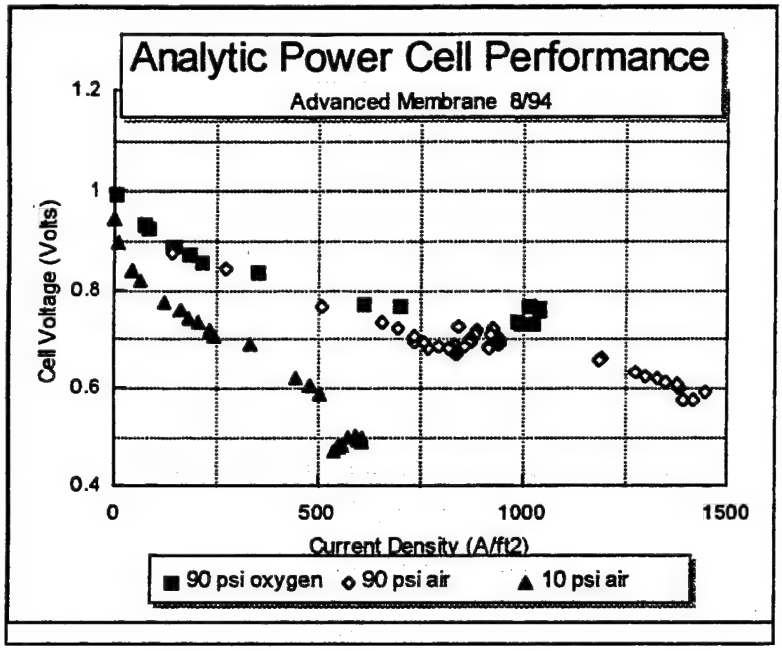

Figure 1 Single Cell Performance - Advanced Membrane

The cell design modifications to produce a planar cell reduced stack resistance from 900 milliohms to 35 milliohms. Performance was increased from 0.5 volts at 30 ASF to 0.7 volts at 65 ASF on hydrogen/air yielding a 5 cell power output of 30 watts. Performance curves for hydrogen/air and hydrogen/oxygen are shown in Figure 2 and Figure 3.

Stack #2 underwent extensive performance testing. During operation the anode showed a temperature rise of up to 60°F. A noticeable amount of condensation formed at the anode exit. We thought that a jet pump, located at the stack inlet, to entrain the liquid water from the exit, would humidify and preheat the anode inlet gas. This would smooth the temperature profile across the stack and improve performance at the inlet side. We installed a jet pump into station 2 of the test stand but we were unable to get results since the stack developed a tear in cell #4 and had to be dismantled.

We also performed a 2 minute load-following test. This test involved varying the load every two minutes then letting the stack remain at a constant load. The load was varied to change the voltage setting from open circuit down to 0.65 volts per cell in 0.05 volt increments. Data was taken at the beginning and end of the two minute period. At each load setting, the current density and voltage increased during the two minute time interval. The stack exit temperature steadily rose. This trend occurred until the voltage reached 0.7 volts/cell. At this point the temperature of the stack was 140°F; but during the next two minutes it rose to 158°F. At the 0.65 volt setting the current density and voltage both dropped and the temperature rose to 181°F. The stack was unable to handle the heat flux and the test was stopped due to the high temperature.

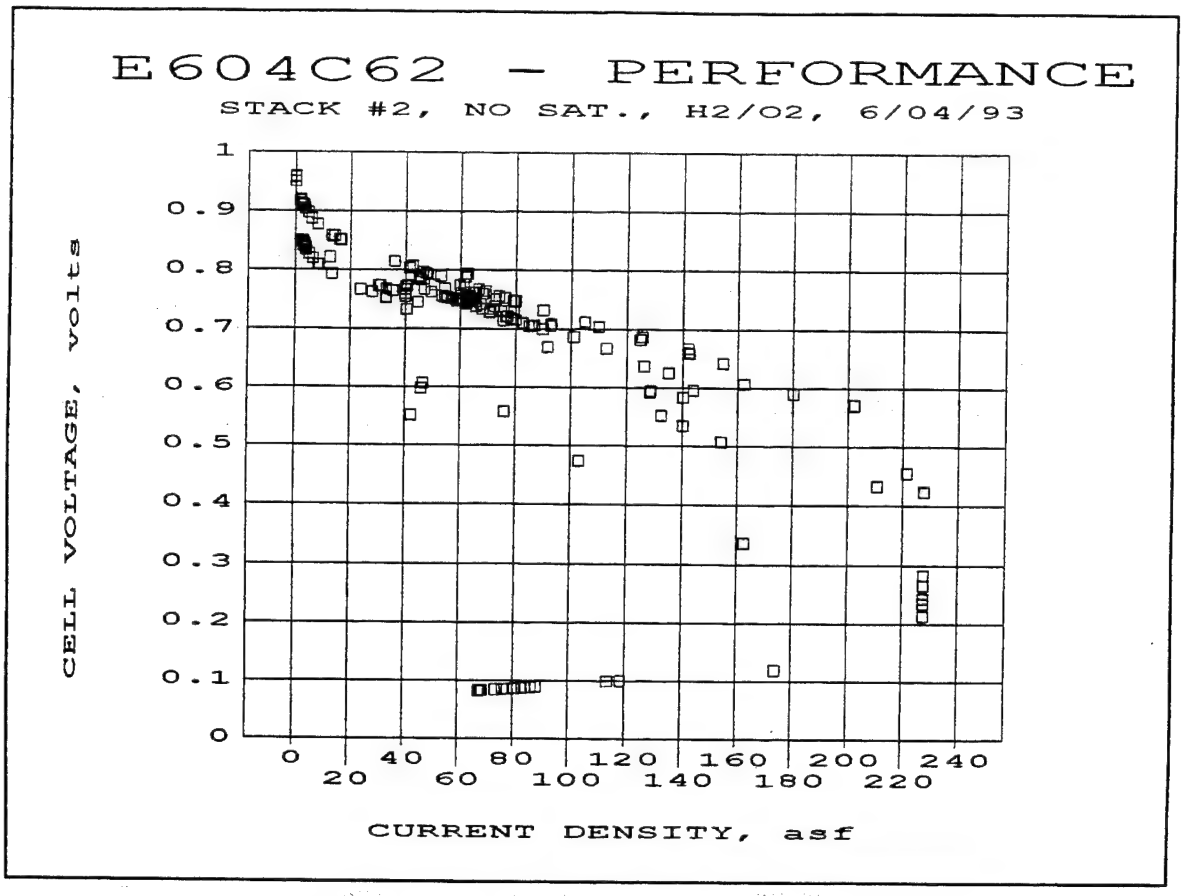

Figure 2 Stack #2 Performance H_2/O_2

When operating the stack with the anode exit port open the stack performance improves with partial inlet anode saturation. Full saturation often floods the anode. Generally, we ran at 50% hydrogen saturation with an 80% utilization. With the anode exhaust port closed the anode gas space retains enough moisture to keep the resistance low. In this case, the stack runs hotter since there is no evaporation of anode side water. The Stack #2 experiments showed that the humidity could be controlled by increasing air utilization but that this conflicted with a requirement to remove heat.

3.1.1.2.2 FC-200

The FC-200, which is a Century Series or Type 4.1.5 fuel cell stack, showed a marked improvement in performance when we reversed the fan flow from "push" to "pull". Figure 4 shows how stack #9 performance varied with the air flow direction in the stack. The straight line of data shows that performance starting at 0.75 volts and 110 ASF falls to 0.6 volts at 90 ASF when fan flow was redirected from "pull" to "push." This drop occurred over a period of one hour and 45 minutes.

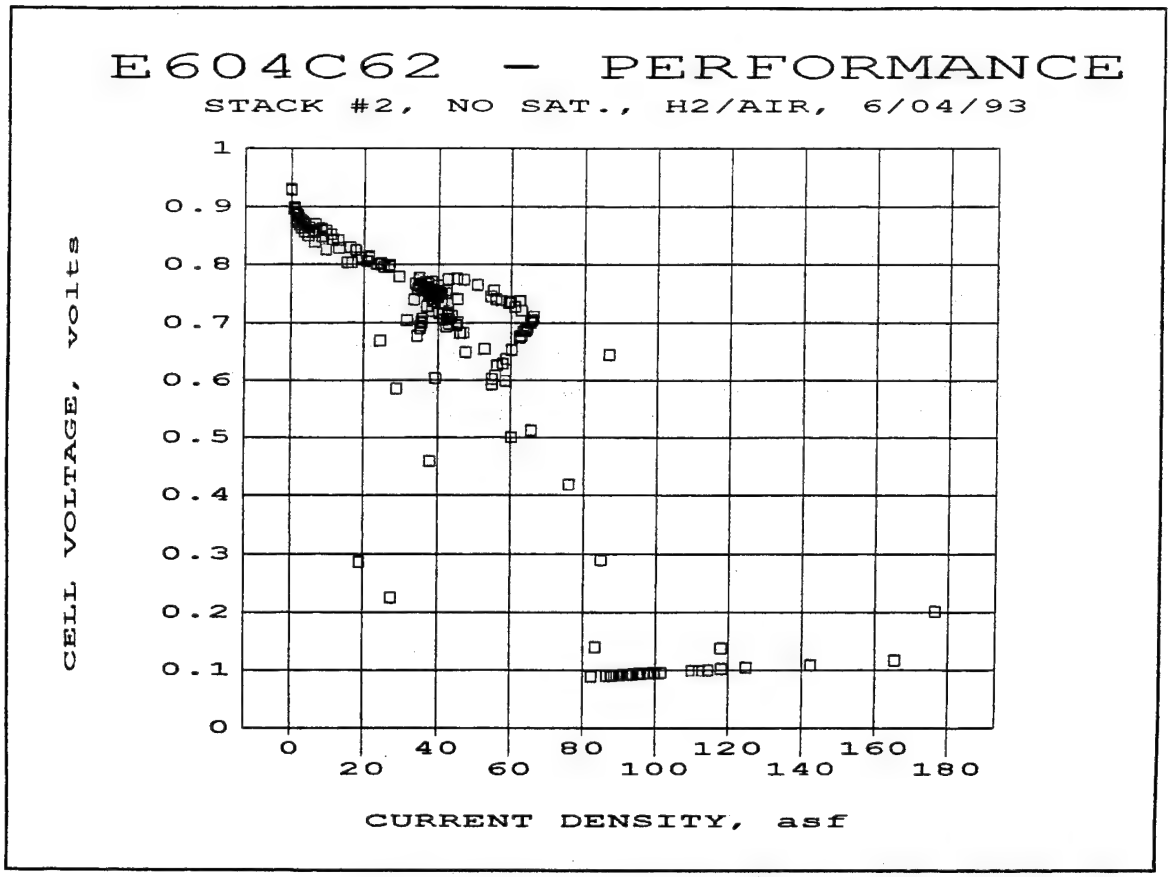

Figure 3 Stack #2 Performance H_2/Air

The same stack with the fan in "pull" mode produced the performance curve shown in Figure 5. Operating in constant current mode, this stack dropped from 0.75 to 0.65 volts at 125 ASF with a maximum post short performance of 0.7 volts at 150 ASF. It produced a maximum power output of 300 watts at 0.56 volts/cell and 225 ASF. One problem with this stack is that the anode space occasionally floods after approximately half an hour. The stack voltage drops to about 0.5 volts. By purging the exhaust port, the accumulated water is entrained in the exit flow and clears the anode gas space. This problem is associated with 2 mil membrane which has superior water transport characteristics.

The control circuits of the stack have become a very important part of its operation. The search for a for flow split control mechanism was initiated with this cell stack. The damper is required because the ratio of cooler to cathode flow rate changes with the power level. We postulated a flow split control with separately ducted manifolds for cathode and cooler air, and a damper valve between the two controlled by nitinol wire. The damper orientation can be controlled by wires in response to the stack current. Start-up may require full flow to the cathode and shut down will require full flow to the cooler.

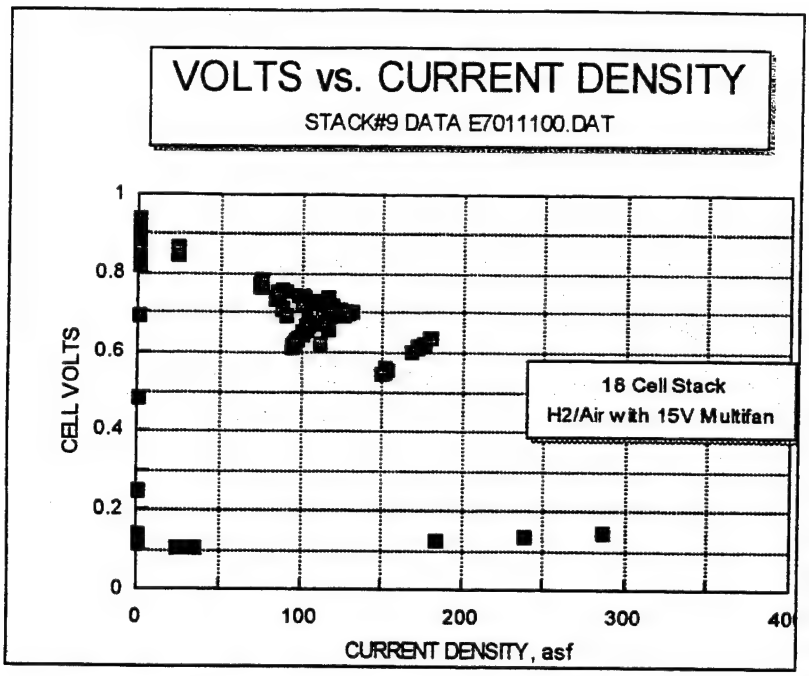

Figure 4 FC-200 Stack #9 Performance with Fan

A delay circuit override may be needed on shutdown. Often during lab testing the stack is operated at full power for the duration of the day. At shutdown the stack is turned off and left dormant. In doing so the stack evaporates water to cool itself since the fan is turned off. This can cause a net loss of water from the membrane. When Nafion is allowed to dry out at high temperature the hysteresis effect prevents achieving that same high performance unless water is introduced again at that temperature. This can be accomplished by shorting the stack. However, if a cell is badly dried out shorting the stack can often result in a negative cell. When and if this happens it can take many hours of operation to recondition the cell. We have started placing the stack in an airtight bag at the end of the day. We also reduce the load on the stack until the temperature is reduced prior to shutdown.

3.1.1.2.3 FC-150

This is a small format (2.5 in x 2.5 in) fuel cell stack designated Type 4.2. Preliminary tests at low currents show most of the 39 cells performing uniformly with the anode exit valve open. Closing the valve causes some of the cells toward the anode inlet side to drop in voltage. These cells may have been severely over-temperatured in the beginning phases of testing. Our understanding of thermal management and air flow is based on the performance of the Type 4.2 stack design, in particular, coupling of the fan(s) with the fuel cell stack. The cell performance is still low. At 100 ASF the cell voltages range from 0.5 to 0.6 volts/cell. The average performance is 0.6 volts/cell at 80 ASF.

The FC-150 performance is limited by its fans running in "push" mode, manifold and cooler flow fields. The stack uses two PeWee Boxer fans operating in parallel. This causes the fans to run at a higher pressure and a lower individual flow. The fans are mounted on the inside of the 2.5" manifold which means they are really only 1.5 inches from the stack surface. This is much too close to achieve uniform flow; a conclusion supported by the data. At low currents, about 40 ASF, the cells appear to be fairly uniform. At higher currents, about 80 ASF, the air flow must increase and specific cells show a marked decrease in voltage compared to their nearest neighbors. These cells are directly underneath the hub of the fans and in the stack center where the flow must branch out to reach these cells. These cells are obviously not getting enough air. By experimenting with different fans, manifolds and flow direction we should be able to improve the performance.

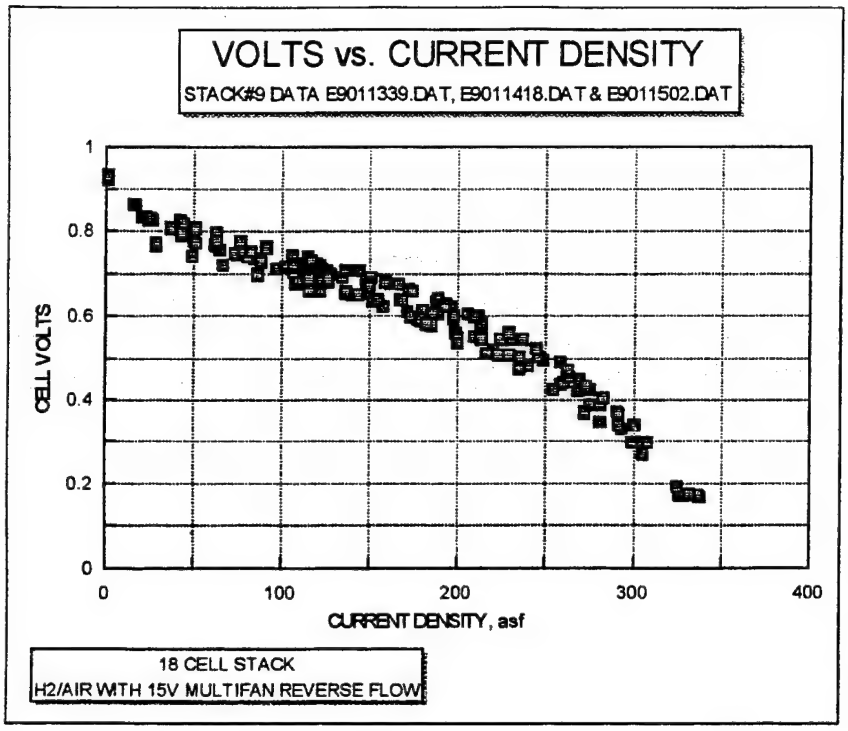

Figure 5 FC-200 Stack #9 Performance with Fan in Reverse

We were unable to run the stack with the exit port closed so all testing was done with a small hydrogen bleed. Closing the anode exit port resulted in a temperature rise in some cells, a sure sign of crossover. We replaced the two large boxer fans with three microfans (approx. 1.5 inches in diameter) at a distance of 2.5 inches from the stack surface. We ran the fans in both directions, pushing into the stack and pulling air through the stack. Neither orientation resulted in any performance improvement. Most fans run with some amount of back flow (stall) when the manifold pressure rise is too high. There is also the possibility of flow maldistribution with fans. This led us to operate the stack with test stand supplied air to determine the air flow requirement.

We used the test stand manifold with a diffuser plate. It was important to eliminate flow maldistribution since this test was to determine the amount of flow for optimum performance and heat management. We ran the stack at varying flow rates to determine the affects on performance and temperature. We also measured resistance. Operating with rig supplied, slightly pressurized air did not increase performance. When operating the stack with the exit port closed the internal temperature of many cells started to rise above the normal of 120°F. The stack resistance was 2 ohms. When compared to the resistivity of the FC-200 the resistance reading of the FC-150 should be about 0.25 ohms or 250 milliohms. The FC-150 resistance is an order of magnitude too high.

All tests indicated that the FC-150 was crossed over. The odd characteristic of the stack is that it had a reasonable open circuit voltage. Stacks with leaking cells usually have a much lower open circuit than we measured. The proof of crossover came when we dunked the stack in a bath of distilled water. Five cells were leaking badly. These cells only leaked when the exit port was closed. The crossed over cells are located in sections where there was a low flow when operated with the original two fan manifold.

3.1.2 Cell Structures

3.1.2.1 Membranes and Resistive Losses

Fuel cell membrane thickness has a powerful effect on thermal management. The fuel cell membrane resistivity (ohm-cm) is a function of its water content. Electro-osmotic drag of water

by protons diffusing from anode to cathode in the cell tends to dry out the anode. The anode in Analytic Power cells is fed by dry hydrogen so that the only means of membrane humidification is via back diffusion of product water from the cathode. Membrane thickness controls the resistance at any water content as well as the back diffusion path length of water replenishing the anode. Thus membrane thickness is of fundamental importance in high performance cell design.

In our Phase I SBIR program we used 7 mil catalyzed Nafion membrane in a 5 cell sub-stack. In a joint program with DuPont, we developed a 2 mil Nafion catalyzed membrane. As predicted, thinner membranes have a higher limiting current density than thick membranes allowing higher power densities. The reduced concentration gradient in the membrane dramatically improved performance.

The cell stack heat management affects the fuel cell performance through the membrane resistance. If a cell is operated at constant load resistance and the membrane dries out the result is high internal resistance. We have observed that cell performance decays along a constant load resistance line to a lower current density and a reduced voltage. The effect is that the cell must remove even more heat to produce power. If the cell or stack hardware cannot keep up with the increased heat flux the temperature increases. This, in turn, dries out the membrane even further.

What we have defined is a thermal instability failure. If a cell is operated beyond its heat rejection limit, it will eventually drop power until equilibrium is reached. If the cell is in a stack and is driven by stronger neighbor cells, it may be driven negative.

We originally observed this effect in our 7 mil membrane, Type 4.1.3 cell size sub-stacks with carbon and plastic bipolar plates. The elimination of metal components served to reduce stack weight but reduced the heat rejection in the stack. This stack achieved 45 ASF at 0.65 volts, but it could not maintain this performance level because of the high temperature. To force the back diffusion of water to the anode and restore performance, we poured water down the cathode flow field channels. In 15-20 minutes the performance would slowly rise but would fall back down as the membrane dried out. In this case, the 7 mil diffusion path length resulted in a large water concentration gradient and anode resistive losses. No amount of cooling will cure this problem. In this case the stack is water transport limited. Only anode humidification or a thinner membrane will solve the problem.

3.1.2.2 Electrodes and Current Collectors

The fuel cell electrode, electrochemically, is the catalyst layer. We also include the carbon paper current collector in the term electrode. The catalyst layer in Analytic Power cells is printed on the membrane, but the carbon paper current collector with a dummy catalyst layer is fabricated separately.

In Analytic Power's large, high pressure, 10 kW fuel cells we employ a dummy catalyst layer to improve electronic conductivity. While these layers are of more benefit at high current densities there are mechanical benefits as well. Originally we used a pitch based Kreha HE-200 material as the current collector. It was used because it has fibers perpendicular to the plane of the carbon paper; so called "z" direction fibers. This particular paper exhibits a large initial load deflection and we rely on compressing the paper from 16 mils to 12 mils. Since the Nafion 112 2 mil

membrane is more fragile than the tough 7 mil Nafion, we expected that the dummy catalyst layer should help prevent the HE 200 current collector fibers from puncturing the membrane. It eventually turned out that the non-linear deflection of the Kreha HE 200 was impossible to fabricate into a planar structure of predictable thickness. This made the printed dummy catalyst layer more important from a conductivity standpoint when the Kreha paper was replaced with Toray TGPH 090.

3.2 Stack Technology

3.2.1 Water and Thermal Management

Early in the Phase II Program we realized that the fuel cell stack was heat transfer limited and we considered raising the catalyst loadings to see if we could improve the cell voltage at low current density. Natural convection stack tests showed that operation was limited to about 50 ASF or lower. Above 50 ASF, the cell temperature rose which caused the cell to dry out and its performance to fall. This is an example of the thermal instability problem we discussed earlier. In Table 1we compare heat rejection in stacks and single cells. The difference between operation in the single cell test rig and operation in the cell stack is that the heat removal system in the single cell test rig is designed to operate at over 5 kw/ft^2 (thermal).

Table 1
Heat Release in Cells and Stacks

	VOLTS	ASF	POWER Watts/ft^2	HEAT FLUX Watts/ft^2
Single Cell Test Stand:	0.8	100	80	45
	0.7	250	175	138
	0.6	400	240	260
25 Watt Cell Stack:	0.6	50	30	32.5

Referring to Table 1 we note that in the single cell test stand, increasing cell voltage has a big effect on heat flux. Raising cell voltage raises cell efficiency and reduces waste heat. A cell stack design which is heat transfer limited can operate at higher power if its efficiency can be increased. Table 1 shows that the limiting heat flux of a naturally convected cell stack about 33 watts/ft^2. Not shown in Table 1, is the present limit for forced air convection cooled stacks which is about 80 watts/ft^2. A very important point in thermal management is that it is imperative that the product water be removed as vapor. If the cathode air flow is so low that the spent air becomes saturated, then condensation within the fuel cell stack will take place. This will increase the heat load on the stack by about 36% at the design cell voltage of 0.7.

3.2.2 Bipolar Plates

Bipolar plates are the most expensive and heaviest components in a cell stack. The design and fabrication of the bipolar plate are at least as important, if not more important than the electrochemical elements. The bipolar plates developed in this program consist of a nitrided titanium gas separator bonded to an ABS plastic frame on the anode side. The cathodes and coolers use ABS hydrogen manifolds and Ultem port bridges. The plastic parts are bonded to the titanium separator with acrylic tapes. The cooler is bonded to a nitrided titanium cathode plate which also has ABS plastic hydrogen manifolds and Ultem port bridges. The anode, cathode and

cooler flow fields are pitch based carbon paper. The carbon paper flow fields are die cut and grooves are machined into the surface with a gang saw developed and constructed during this program.

3.2.2.1 Anode Frame

The anode frame is an injection molded ABS plastic part . It forms a frame around the anode flow field and supports the anode seal. Ports from the hydrogen manifolds to the anode flow fields are integral with the frame. With the reduction in membrane thickness came a reduction in the unitized cell edge thickness. We use a mylar shim the same thickness as the membrane in the sealing surface. Initially, the reduced membrane thickness caused a loss of stiffness in the cell frame resulting in anode manifold gas leaks. While the 7 mil membrane cell package sealed in the stack hardware the 2 mil membrane package did not. Upon teardown we noticed rippling of the mylar cell frame in the region of the manifold slot where the frame bridges the grooved anode flow field. The frame is unsupported at each groove and the loss of sealing pressure allows gas to escape from the anode manifold through the glue layer and into the cathode gas space. The result is a sealing loss with a large drop in open circuit potential and performance. We have seen this effect before across the cathode flow field grooves in our phase I program.

One solution is to increase the thickness of the mylar electrode frame to 0.014 inches to increase its stiffness. However, this requires a thicker electrode material of PAN fiber. Pitch fiber electrodes are not available in this thickness. Also, it did not solve the problem of anode flow field crumbling in the port region. At any point where a grooved flow field crumbles there is a loss of sealing surface which is a source of gas leaks. Moreover, the loss of sealing pressure tends to be transmitted to surrounding cells.

We modified the anode ABS injection molded frames to eliminate the flow field material from the sealing surface. In order to port the hydrogen from the manifold slot to the anode gas space the ABS frame has to be grooved to mate with the grooves in the flow field. The frame grooves face the bipolar separator plate so that the mylar cell frame will seal against a flat surface. A 15 mil thick piece spanning a 100 mil groove width at a contact pressure of 180 psi is subjected to a tensile load of over 6,000 psi. Since the tensile and flexural strength of ABS plastic is 45,000 psi and 76,000 psi respectively, the frame is strong enough to prevent the mylar from rippling and losing its seal.

With this design it is important to have an accurate grooving machine to ensure that the grooves in the ABS and the flow field line up. The channel area in the port was reduced causing an increased pressure drop. However, this is advantageous since we would like a higher port pressure drop and a lower flow field pressure drop to improve anode gas distribution.

We had several anode frames machined with these grooves and placed in a small sub-stack for seal testing prior to modifying the injection mold. The ported anode frames used in Stack #1 and Stack #2 were machined rather than injection molded to determine their effectiveness. The machined anode frame was made without alignment rings to reduce cost. This eliminated the movement restriction placed on the long frame edge. During stack pressing the long frame span bulged outward placing a tensile stress on the membrane. This in turn forces the short sides of the stack inward. If the frame moves outward more than 1/8th of an inch the cell becomes

unsupported at the electrode frame interface and becomes susceptible to crossover or tearing. This tearing is what happened to cell #4 in Stack #2, our 5 cell sub-stack.

3.2.2.2 Port Bridges

Results from Stack #2 show that porting the anode and cathode flow field frames works well. Eliminating the carbon paper from the seal region allows a higher contact load without crushing the carbon and losing seal integrity. A further advantage is that the mylar electrode frame thickness can be reduced since the mylar is supported across the channel groove by the port bridge. This in turn permits a reduction in the electrode thickness which has a direct affect on the performance of the cell. A reduction of the cathode electrode thickness in particular significantly improves performance by decreasing the oxygen diffusion path to the membrane surface. The advantages are won at a great cost as the cathode and cooler port bridges are the single most expensive elements in a fuel cell stack. The use of roll fins to replace the plastic port bridges should resolve the high cost of plastic parts.

3.2.2.3 Metal Gas Separators

Metal gas separators were used when we discovered that the Phase I carbon paper and plastic bipolar plates leaked. We first tried titanium foil separators which oxidized. We next used stainless steel. Stacks were made with 0.005" thick stainless steel separator plates. The port bridge design provided a 0.015" span across the channel groove on both the anode and cathode. The mylar thickness was reduced from 0.014" to 0.007". The electrode thickness was reduced from 0.012" to 0.010" with a dummy catalyst layer added on the membrane side to improve contact resistance. The separate cell package design was eliminated and replaced with just a membrane supported by the electrode across the flow field/port bridge seam. A springy carbon shim was placed between the metal separator and the carbon flow field and the adhesive was removed from this region.

The original reasons for using metal in the bipolar plates was to eliminate the bipolar plate gas crossover which was a problem in phase I. The steel separators also alleviated the propagation of cathode flow field crushing in the port region. The next reason for using metal plates was to add stiffness to the fuel cell stacks. Prior to using plastic cathode ports, flow field crushing of the Kreha carbon paper flow fields in the cathode ports was a severe problem which led to hydrogen leakage.

We used acrylic tape between the carbon paper flow field and the stainless steel. The carbon paper was pressed through the acrylic. Experimental studies showed that this was a major source of stack resistance.

Heat rejection had been shown to be the difference between operating at a power density of 240 watts/ft^2 rather than 30 watts/ft^2 at the same potential. Our early stack designs used free convection cooling and in order to passively control the heat we need to add more heat transfer surface to the stack. We also hoped to improve heat removal by extending the steel fin past the manifold edges. Stainless steel fins were inadequate in this application.

Rather than die cutting or machining, the plates were laser cut which increases the fabrication cost. Because we have not fixed the specific cell size, we have not committed to a low cost fabrication method such as die punching or EDM.

Titanium nitride was identified as a low cost, protective coating material. We have considered switching from titanium plates to stainless steel or aluminum as our separator plate material. Stainless steel is about twice as dense as titanium and adds weight. Aluminum is light in weight and has a much higher electronic conductivity. Aluminum is more reactive than either titanium or stainless steel, and prone to form non-conductive oxides in the presence of water. Aluminum and steel can be protected with coatings of titanium nitride but the coating is expensive. Inexpensive titanium coating procedures on titanium base metal, developed in this program, make titanium plates the material of choice.

3.2.2.4 Flow Fields

The flow fields of the cell distribute reactant gases over the surface of the cell. They also keep droplets from forming in the gas distribution grooves and manage liquid water within the reactant gas spaces. Liquid water will occasionally be present in the reactant spaces adjacent to the cells. Provision must be made to accommodate and remove liquid water within the cells. Early in the Phase II program, Analytic Power discovered that it is possible to render carbon paper flow fields hydrophilic by anodically evolving oxygen from the surface of the flow field while it was in an acid bath. This treatment, by itself, is helpful in keeping the flow field grooves clear of water. In forced convection cooled cells, it is inadequate to accommodate and dispose of the product water. We have also found that the improvement in wetablility is temporary. Wicks can be expeditiously placed between the cathode flow field and the cooler flow field. The high air flow rate of the cooler tends to dry the wicks and removes excess water from the cathode flow fields.

Flow fields, especially the cathode air and cooler flow fields control the split between these gas streams. They are also the thickest members in the cell stack and contribute directly and indirectly to the size, weight and cost of the cell stack. During the course of the program it became apparent that the cell stack size and cost were limited by the carbon paper flow fields. After the port bridges, the flow fields are the most expensive item in the cell stack. Because of their low shear strength, gas passage grooves occupy only 50% of the cross-sectional flow area. Roll fins developed in the last six months of the program have made the carbon paper flow fields obsolescent.

3.2.3 Follow-up Systems

The follow-up system consists of end plates, tie rods and current collectors. The function of the follow-up system is to maintain seal integrity, to minimize contact resistance and collect the current from the cell stack. The follow-up system is the heaviest portion of the stack.

The end plates used in all of the prototype stacks in this program have been G10 fiberglass. The end plates were designed using finite element software. The tie rods have varied in size and number but they have been located outboard of the cell frame. In this configuration, the moment on the end plates tends to place very heavy loads on the cell frames. The rotation also tends to unload the centerline of the cell stack. Prior to the use of Ultem port bridges, the end plate loads tended to crush the cathode flow field ports. This warped the end plates into a saddle shape. The

use of plastic port bridges and flow field shims have solved these problems. When a stack is compressed, the cells between the end plates are completely flat.

3.3 Systems Technology

3.3.1 Gas Flow Distribution

3.3.1.1 Pressure Drop Analysis

A pressure drop analysis of the hydrogen and air sides was performed on FC-150 and FC-200 stacks. The pressure drop was based on the laminar flow equation (Hagen Poiseuille) since the Reynolds numbers never exceeds 200.

The FC-150 hydrogen side pressure drop is 0.153 inches of water which is insignificant since the hydrogen inlet pressure is generally 5 psi. The only important factor is that the port pressure drop is at least an order of magnitude higher than the manifold pressure drop. This aids in uniform reactant access to each cell in the stack.

The air side pressure drop is much more significant. Separate calculations were done on the reactant and cooler ports. Form drag as well as frictional drag was taken into account. The form drag exceeds the frictional drag. Prior calculations only considered frictional drag. The form drag is based on inlets, exits, flow restrictions and expansions and turning losses. Form drag is a function of the square of the flow velocity. Turning losses have the highest drag coefficients.

Volumetric flows on the air side were calculated assuming a 40% utilization at a performance point of 120 amps/ft^2. The cooler side flow was determined based on a stack convective heat transfer analysis. Cooling flows are about 15 times that of the reactant flow. With this flow through the coolers we can calculate the pressure drop. For the FC-150 the reactant pressure drop is 0.227 inches of water and the cooler pressure drop is 1.973 inches of water. Since we know that the fans we are currently using on this stack are capable of, at most, a 0.3 inch of water pressure rise, the FC-150 cooling flow is not sufficient to maintain heat balance. The reactant pressure drop is just about at the maximum rating of the fan. This could mean that some amount of evaporation is taking place within the stack. The stack is most likely operating at very high reactant air utilization and running hot. Lab testing has shown this to be the case. These calculations also tell us that the flow split between cooler and reactor is approximately 2 to 1 when it should be approximately 15 to 1.

The FC-200 has a similar problem but to a lesser extent. The reactant pressure drop is 0.178 inches of water and the cooler pressure drop 0.869 inches of water. This stack has a better chance of maintaining its heat and water balance. There may be a small amount of evaporative cooling but the stack has plenty of reactant air and the flow split is approximately 3 to 1.

Operating this stack with the fans further complicates this issue. If the fans are incapable of delivering the needed pressure rise, backflow (stall) occurs. This makes it virtually impossible to determine the air flow of the stack. Our modifications to the test rig should allow us to directly measure the flow rates. However, increasing the flow through the stack may allow too much flow

to pass through the reactant channel and not enough flow to go through the cooling channels unless we can control the flow split.

3.3.1.2 Air Management & Fans

Low flow fans (under 30 SCFM) generally have a maximum pressure rise of 0.2-0.4 inches of water. This doesn't leave many options for cooling.

We tested several fans and fan manifold arrangements. Blowers are a high pressure option but they are large noisy and inefficient.. Cross flow fans or blowers may be an option. A cross flow or tangential fan is long and narrow. The flow orifice extends the entire length of the small diameter impeller. This should yield a low profile manifold. We have identified one cross flow fan that is compatible with our flow and size requirement. Unfortunately, the transaxial flow fan has a low pressure rise, and tends to be noisy and inefficient. For example a 2.6 watt Panasonic fan has a pressure rise of about 0.06 inches of water and a noise level of 38.2 dB-A.

The rule of thumb is that the fan should not be closer than one and half a fan diameters to the stack surface. Using many microfans may reduce the depth of the manifold and help distribute the air through the stack. The microfans are 1.5" square by 3/8". Three fans at 3.5 cfm each should suffice for an FC-150. During testing we found that the stack had other problems (crossover) so we were not able to obtain meaningful results.

Fans with a large hub diameter require placement further away from the stack. This is due to the resulting cone of inactivity, or shadow, in front of the hub. Our FC-200 appears to have this problem. We switched from a 3.2" square PeWee Boxer fan to a 3.6" square 15V multifan for our latest design. The multifan was chosen for its higher pressure rise, larger size and capability of running at different voltage levels. The voltage range came into play when we started using the fan circuit which varies the voltage based on stack temperature. Running for long periods at other than rated voltage can cause motor burnout. The larger size was advantageous in providing air to the end cells. This fan provided more flow to the edge cells. However, since the fan was placed the same distance from the stack surface, the center of the stack heated up. The cooling flow in this region was insufficient and the stack performance dropped.

The FC-200 stack had poor cathode flow distribution. This was difficult to determine at first because the overall stack resistance was low. We tested the temperature distribution at the surface and at various points in the air flow passage through the operating cell stack. This maps the effect of flow distribution on stack performance. A thermocouple registered a 20 degree temperature difference between the center of the stack and the surrounding one inch radius. The stack center was 140°F compared with the stack perimeter temperature of 100 °F. There is no simple way to measure the localized resistance of a cell. The upper and lower region of the cell may have had sufficient water but the center was most likely dried out.

Air flow tests determined the areas of greatest flow and the "dead" zones; those with little or no air flow. We used a thread on the end of a wire probe to determine the manifold air flow direction. We tested an angled manifold with the PeWee Boxer fan and the rectangular manifold with the multifan disconnected from the stack. The fan was connected so the air flow was directed into the stack. In both manifolds the upper and lower two inches had no flow. The center section

showed circular flow. The required distance from the multifan for smooth flow at the hub was 4.5 inches. Connecting the fan manifold to the stack resulted in a broader flow area but more turbulence. Flow in many of the regions was sideways or backwards toward the fan.

Moving the fan further back would have increased the volume and weight of the stack which is counterproductive. Running the fan in reverse or pulling the air through the stack improves performance since the stack acts as a large flow straightener. The other advantage is that the fan can be located a closer to the stack surface. The only concern is the lack of a wick in the back cathode port bridge. This area can sometimes get clogged with water drops causing an increase in pressure drop through the cell.

3.3.1.3 FC-150 Pressure Drop Testing

In order to quantify the problems of the FC-150 we needed to better understand the air side characteristics. Since the fan flow cannot easily be measured we connected the stack to the test stand air supply. We constructed a manifold to distribute the air flow evenly across the stack surface. This manifold was used for performance and pressure drop testing. The manifold was simply a Plexiglas box between rig and stack that contained a diffuser plate and ports for a manometer tube.

We measured the pressure drop on the air side with a manometer at flow rates from 1 to 3.5 scfm. To measure above 3.5 cfm we will need to change some gages on the rig. We constructed sensitive manometer using water in a U-tube at an angle of 15°. This apparatus proved useful and we took flow and pressure drop readings with the stack dormant.

We took three separate sets of readings. One set with cooling channels blocked and reactants open; one set with cooling channels open and reactants blocked; and one with both open. Each set consisted of 3 different readings at 5 flow conditions of 0, 1, 2, 3 & 3.5 cfm. The three readings were taken at different port locations in the rig manifold spaced evenly along the length of the stack. The reading at the zero flow condition was to calibrate the manometer. The results in Table 2 show the raw data and pressure drop.

Our test results correspond fairly well with our calculations. The spreadsheet calculations show that at a flow rate of 3 cfm through the coolers the resulting pressure drop should be about 0.69 inches of water. The average of our readings at this condition is 0.68 inches of water. The reactant pressure drop assuming a 40% utilization should be 0.22 inches of water at a flow of less than 1 cfm. This calculation is a little high since our readings indicate a 0.08 inch of water pressure drop. However, the accuracy of the readings diminishes at lower flow rates since the movement of the water level is smaller.

The test results indicate that we may be getting enough reactant air through the stack but not enough cooling air. To develop a pressure rise above 0.3 inches of water we will need a blower. A fan is not capable of cooling this stack.

Table 2

RAW DATA						PRESSURE DROP			
REACTANT AND COOLING CHANNEL									
	CFM					CFM			
PORTS	0	1	2	3	3.25	1	2	3	3.25
1	20.56	20.63	20.69	20.88	20.88	0.081	0.163	0.406	0.406
2	20.56	20.63	20.69	20.88	20.88	0.081	0.163	0.406	0.406
3	20.56	20.63	20.69	20.81	20.88	0.081	0.163	0.325	0.406
COOLING CHANNEL OPEN/REACTANT									
	CFM					CFM			
PORTS	0	1	2	3	3.25	1	2	3	3.25
1	20.50	20.56	20.81	21.13	21.19	0.081	0.406	0.813	0.894
2	20.69	20.69	20.81	21.13	21.13	0.000	0.163	0.569	0.569
3	20.63	20.63	20.81	21.13	21.19	0.000	0.244	0.650	0.732
REACTANT CHANNEL OPEN/COOLER									
	CFM					CFM			
PORTS	0	1	2	3	3.25	1	2	3	3.25
1	20.50	20.56	20.88	21.63	21.81	0.081	0.488	1.463	1.707
2	20.38	20.38	20.56	21.19	21.44	0.000	0.244	1.057	1.382
3	20.50	20.63	20.94	21.63	21.75	0.163	0.569	1.463	1.626

3.3.2 Thermal Management Alternatives

Heat rejection is the difference between operating at a power density of 240 watts/ft^2 rather than 30 watts/ft^2 at the same potential. The only way to reduce the size of the present fuel cell stacks is to use higher overall heat transfer coefficients within the cell stack. Heat rejection to the atmosphere will always be a size limiting consideration in mobile power applications. However, it is still possible to reduce the stack size considerably by using liquid or two phase heat transfer coefficients within the cell stack.

3.3.2.1 Natural Convection Analysis

At the Power Sources conference we delivered a paper which discusses the results of our natural convection cooling experience in detail. The single cell experiment discussed in Section 2.4.2.2 is repeated at the stack level and the results are given here. The problem with natural convection is the effect of high temperature on the Nafion membrane. The important point here is the presence or absence of water. A temperature rise will directly improve performance. However, if the stack is allowed to heat up in a dry cathode stream, the membrane resistance rises dramatically, creating more heat. This triggers a higher flow rate through the cathode to conduct away the heat exacerbating the evaporation of water from the membrane. Increasing the stack temperature by shorting is usually benign since it forces the production of water at the cathode.

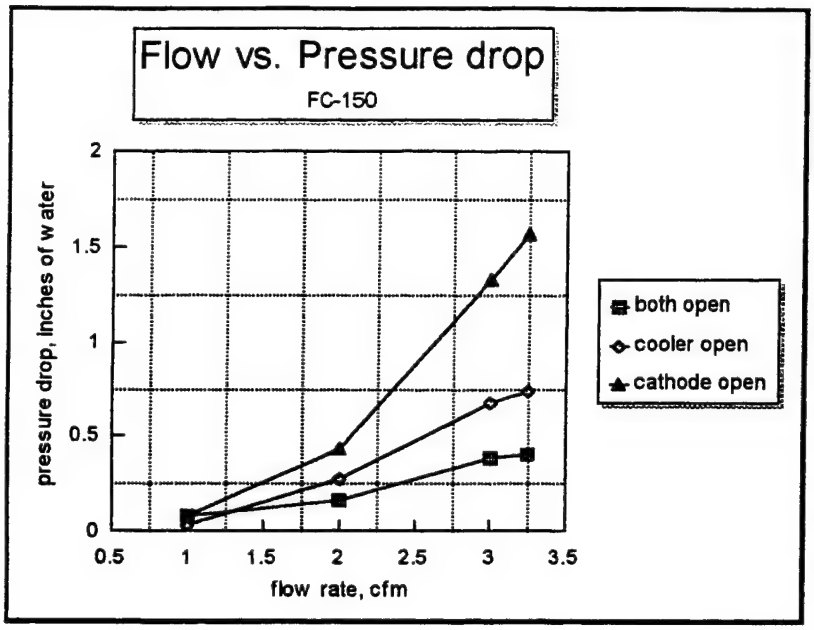

Figure 6

Figure 7 and Figure 8 show plots of temperature with voltage and temperature with current versus time. The stack was operating on hydrogen/air without saturation under natural convection. The figures show that when running at voltages above 0.7 volts/cell the stack performance is steady and the temperature line is flat at about 115°F. At high voltage the stack operates more efficiently creating less heat in the process. After 40 minutes of operation the stack was shorted briefly. This brought the current up from 5.5 amps to almost 9.0 amps or about 68 ASF at 0.7 volts. The stack was producing over 31 watts. The voltage was set at 0.7 volts and the stack was allowed to sit undisturbed for about an hour. During this time the stacks temperature rose by 45 °F. At a lower voltage the stack creates power less efficiently and cannot sustain itself as is evidenced by the simultaneous drop in voltage as well as current. The performance increase due to temperature rise is overshadowed by the performance drop due to membrane water loss.

To reduce the temperature the stack was left briefly on open circuit and then the voltage was set to 0.75 volts. The temperature rapidly dropped to 140°F then slowly dipped to 120°F. Although the performance was steady it was at a lower point. There was permanent water loss at the high temperature resulting in a higher membrane resistance. This is due to the Nafion hysteresis effect. To recover performance the stack must be run at high temperature in the presence of water. This can be done by running the cell on saturated gas or shorting.

The flip side to the above problem is operating at a point in which the temperature is too low or the heat release too small. In this case, there is an insufficient driving gradient for flow through the cathode. Water production is greater than the evaporation through the cathode and flooding may occur. Since the reactants have to diffuse through the liquid water the partial pressure is reduced and so is performance. The net affect is the same as with high temperature. We have seen this affect when operating in station 2 under very high air utilizations.

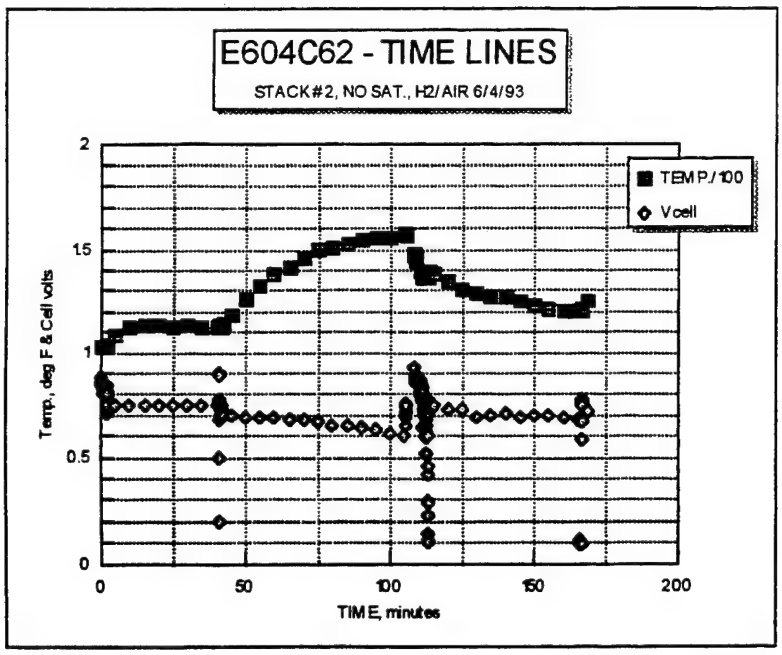

Figure 7 Stack #2 Temperature with Voltage

These trends have also been demonstrated by our single cell testing as well as our 25 watt stacks. Stacks with a high resistance cannot sustain performance. Stacks with a low resistance can sustain performance as long as the air flow and heat removal are controlled for varying load conditions. Our results show that there is an optimum operating temperature surface based on the stack's internal resistance. Stack #2 showed that you must run at the stacks heat removal capacity which may be done by setting the right cathode flow and cell voltage.

3.3.2.2 Single Cell Test Results & Data Analysis

Early in the program, a single cell experiment was performed which defined our current understanding of the effect of heat management on cell performance. A single cell was prepared using a 40% wt Pt on Vulcan XC-72 catalyst (E-TEK) having a total catalyst load of about 0.53 mgm/cm^2. This compares to our present 20% wt Pt on Vulcan XC-72 (PMC) with a loading of about 0.2 mgm/cm^2. The cell had an area of 5.06 in^2. It was first tested on 9/25/92 at high pressure and temperature where it performed about as well as prior cells. It did not "breathe" well and was characterized by relatively high air/O_2 gains and a limiting current density of about 3500 ASF (H_2/O_2). It had a somewhat elevated resistance of about 4.5 milliohms. Its performance at 0.7 volts was a respectable 800 ASF (H_2/air).

After remaining overnight in the high pressure test rig, the cell was started on 9/26/92. On hydrogen and air, ambient pressure and temperature, its performance was steady for 2.5 hours at 400 ASF and 0.5 volts. During this time its temperature never rose to more than 110^{o}F. The temperature time history is shown in the Figure 9.

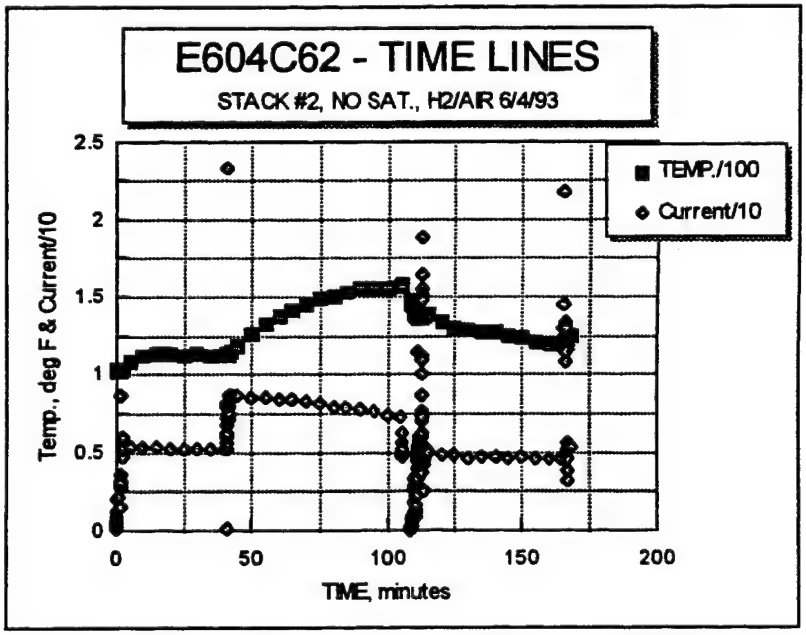

Figure 8 Stack # 2 Temperature with Current

The current during this time is also shown. Note that a current of 15 amp is equivalent to about 430 ASF. Figure 10 shows the cell voltage history.

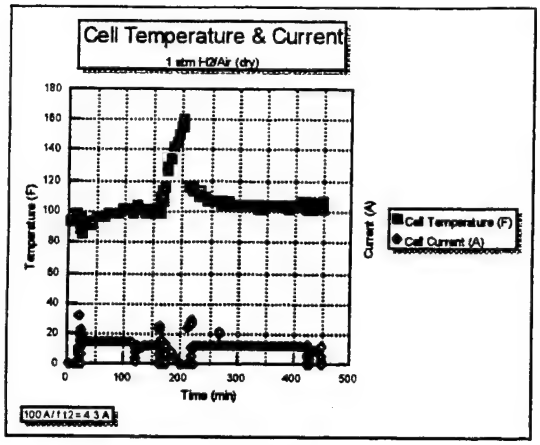

Figure 9

After operating at a steady rate for about 2.5 hours, we increased the operating temperature of the test rig to 155°F. The results of the temperature transition are clearly illustrated on Figure 9 and Figure 10. The result was that the cell resistance rose from about 4.5 milliohms to about 687 milliohms. The limiting current density fell from about 900 ASF to 23 ASF. The reason for the decline is the loss of water from the membrane. Water plays an important role in both membrane resistance and electrocatalysis.

After operating the cell at this condition for several minutes, we cooled the cell to about 110°F in twenty minutes. During this time we operated the cell at short circuit. We did not use the saturators to externally saturate the inlet reactant hydrogen. The cell product water permitted the cell to recover its performance. The "restored" performance line can probably be raised by completely saturating the membrane.

We refined our thermal model to quantify the relationship between heat generation and temperature profile across the stack. This affects membrane water loss changing resistance and therefore stack performance. With a working model we can better understand the performance characteristics of the stack. We generated a cell temperature profile that approximately predicted the actual cell temperature profile in an operating stack curve.

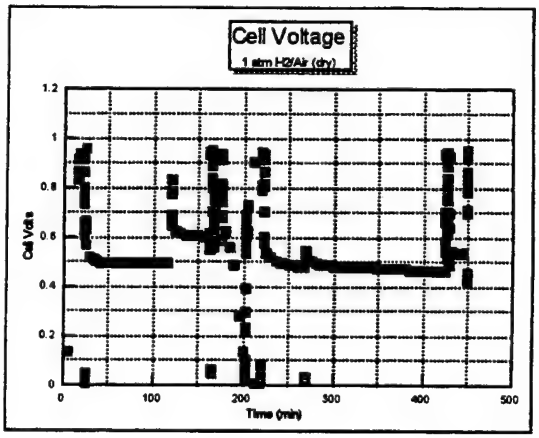

Figure 10

3.3.2.3 Forced Convection Stack Design

Forced convection and recycle provides independent control over heat removal and water management. Analysis of the natural convection characteristics points up the importance of changing to a forced convection design. Forced convection makes the stack independent of orientation and immune to contaminants. It also decreases the cell pitch and improves heat transfer. This, in combination with an anode recycle arrangement, can provide the moisture needed to run a hydrogen generator as well. Such a stack will have reactant counter flow and internal manifolds. We have a preliminary design based on our heat exchanger work

3.4 Fuel Source Technology

3.4.1 Hydride Research

In researching chemical hydrides, Sodium Borohydride($NaBH_4$)seems to be best suited for our application. The reasons $NaBH_4$ is such a good candidate is because of its low cost and its high hydrogen ratio. The reaction is:

$$NaBH_{4\,(3)} + 2\,H_2O\,(L) \rightarrow 4\,H_2\,(g) + NaBO_{2\,(3)} \qquad \text{High Temp.}$$

$$NaBH_{4\,(3)} + 4\,H_2O\,(L) \rightarrow 4\,H_2\,(g) + H_3BO_{3\,(3)} + NaOH\,(aq) \qquad \text{Low Temp.}$$

The heat of reaction is -15.06 Kcal/mole H_2. The weight to hydrogen ratio is 0.4221 grams of $NaBH_4$ to 1 liter of hydrogen. The product of the $NaBH_4$ and water reaction is $B(OH)_3$.

The problem with using only $NaBH_4$ and water is that the reaction is pH dependent. This means as the reaction goes towards a basic pH the reaction slows down. A pH of around 4 - 5 drives the reaction to completion. The reaction is pH and temperature dependent. Both Co and Fe are known catalysts for the reaction.

3.4.2 Reactor Test Stand

The test stand was designed for testing solid and liquid chemical hydride sources. The reactor vessel is rated to 1500 psi(max.) and is chemically stable. The vessel is also fitted with a thermocouple feed through for up to 4 thermocouples to measure local temperature distributions within the reactor. The vessel is made of 304 stainless steel and has an internal volume of 1 liter. The test stand is able to measure flow rates up to 5 SLPM. It is also equipped with two cooling systems, one for the exiting hydrogen and the other for the reactor shell. Water is supplied to the reactor through a pressurized reservoir on the test stand. A back pressure regulator was added to keep the reactor pressure stable while adding water. The flow rate, pressure, temperature and time are all recorded through a Data Acquisition and Control (DAC) program.

A die was made for molding the $NaBH_4$ powder mixtures. This die is used in fabricating 2" x 2" corrugated pucks.

3.4.3 Material Selection

The Fuel consists of a chemical hydride, a salt of acid anhydride and a binder, usually epoxy. Sodium Borohydride, as stated was best suited for this application. The selection of a catalyst or pH controller for this application includes Aluminum Chloride($AlCl_3$), Phosphorus Pentoxide(P_2O_5), and Cobalt Chloride($CoCl_2$). Our initial tests were performed using $NaBH_4$ and P_2O_5 mixtures in a "puck" form. These pucks exhibited high heat releases and were very difficult to control. Other tests were done on $NaBH_4$ & $CoCl_2$ pellets yielding similar results.

The problem related to these chemicals are high heat releases and hydrate formation on the solid surface. The Mixture of $NaBH_4$, P_2O_5 and H_2O yields a heat release of -49.56 Kcal/mol. The reaction looks like this:

$$\begin{aligned} NaBH4\,(c) + 1/6\,P_2O_5\,(c) + 3.5\,H_2O\,(L) &\rightarrow 4\,H_2\,(g) + B(OH)_3 + 1/3\,Na_3PO_4 \\ + 2.5\,H_2O\,(L) &\rightarrow 4\,H_2\,(g) + HBO_2 + 1/3\,Na_3PO_4 \\ + 1/2\,P_2O_5\,(c) + 3.5\,H_2O\,(L) &\rightarrow 4\,H_2\,(g) + HBO_2 + NaH_2PO_4 \end{aligned}$$

Hydrate Form: $Na_{(x)}\ H_{(x)}\ PO_4 + (n)\ H_2O \rightarrow Na_{(x)}\ H_{(3-x)}\ PO_4 * n\ H_2O \quad n=0,1,2,...$

The reaction set equation shows three different product, each having different heat releases. This makes controlling the rate of reaction very difficult, since it is pH and heat dependent. The reason P_2O_5 is attractive for this system is its affinity for water. The high reaction temperature causes rapid expansion of materials and increase rate of reaction . These have an autocatalytic effect making the control system complex.

The combination of $NaBH_4$, $AlCl_3$ and H_2O yields a heat release of -12.6 Kcal/mol. This reaction not only has a lower heat release but also yields only one set of products. The reaction products are 4 H_2 , aluminum hydroxide, and common salt (NaCl).

Hydrates are formed in each of the different mixtures. They appear as a crust on the surface of the substrate. The hydrates are water soluble, but need a large excess to be effectively removed. The structure and composition of the fuel can reduce the size of the hydrates. The hydrates form slower if the inlet water is supplied at a constant rate. This causes the hydrate to dissolve before it has a chance to grow. The hydrates require excess water. Large pulses of water make the hydride expand rapidly, reducing the water required to sustain the hydrogen production reaction. The hydrate forms a hard shell. This hydrate acts as a barrier between the incoming water and the borohydride. The barrier is temporary until the hydrate dissolves, but it does delay the reaction.

3.4.4 Puck Research

The mixture of two or more powders and the addition of a binder pressed into a desired shape is what we call a puck. Several different binders were tested for chemical stability, work life, hardness, and strength. The first binder used was a 3M epoxy (DP-270). This epoxy has a 90 minute work life and is used primarily for potting electrical components. The long work life makes manufacturing the pucks difficult. In manufacturing pucks, a 2" x 2" die is used to mold the material into a corrugated configuration. Since the work life of the epoxy is a problem, we tried a faster curing epoxy. This epoxy , also from 3M(DP-100) has a work life of 3-5 minutes. The much faster hardening epoxy didn't leave enough time to work with the puck material. The DP-100 epoxy also reacted with the P_2O_5 over a short period of time. The next epoxy 3m (DP-110), has a 10 minute work life and it doesn't react with the puck materials.

The puck design is complex. The structure has to be strong enough to prevent disintegration during reaction. The reaction creates large internal forces with high local temperatures. The puck must also be hydrophilic. When a drop of water contacts the pucks surface it is absorbed. The reaction between the water and the $NaBH_4$ generates hydrogen.

Reaction of NaBH4 in excess water:

	$NaBH_4$		$\rightarrow Na^+ + BH_4^-$	(Ionization)	1
	BH_4^-	$+ 4\ H_2O$	$\rightarrow B(OH)_3 + OH^- + 4H_2$	(Hydrolysis)	2
	Na^+	$+ OH^-$	$\rightarrow NaOH$	(Dissociation)	3
	H_3BO_3		$\rightarrow HBO_2 + H_2O$	(Dehydration)	4
	$2\ HBO_2$		$\rightarrow B_2O_3 + H_2O$	(Dehydration)	5
Net:	$NaBH_4 + 4\ H_2O$		$\rightarrow 4\ H_2 + B(OH)_3 + NaOH$	(without dehydration)	

The addition of the acid anhydride or salt helps tie up Na^+ ions to keep the pH low. We add acetic acid to lower the pH of Rx 2-3 which will otherwise shut down the hydrogen evolution.

$$CH_3COOH + Na^+ + OH^- \rightarrow CH_3COONa + H_2O$$

The same can be done with other acids (HCl, HNO_3, H_3PO_4), acid anhydrides ($(CH_3CO)_2O$, P_2O_5), or salts of strong acids ($CoCl_2$, $AlCl_3$).

Test 1

The purpose of this test is to see how the reaction acts with varying amounts of $AlCl_3$ in the puck. Three pucks were made each having equal amounts of $NaBH_4$ (5 grams). A stoichiometric amount of water is added to each puck.

Puck #113 is made with:
5 grams of $NaBH_4$ (66%)
1 gram of $AlCl_3 * 6 H_2O$ (13%) , (9% of stoichiometric)
1.5 grams of epoxy (20%)

Puck #114 is made with:
5 grams of $NaBH_4$ (25%)
11 grams of $AlCl_3 * 6 H_2O$ (55%) , (stoichiometric)
4 grams of Epoxy (20%)

Puck #116 is made with:
5 grams of $NaBH_4$ (18%)
16 grams of $AlCl_3 * 6 H_2O$ (62%) , (150% of stoichiometric)
5.375 grams of Epoxy (20%)

Theoretically each reaction should act differently. Puck #113's reaction should be slow and fall off quickly because of the lack of acid to drive the reaction. Puck #114's reaction should be fast and steady and fall of gradually, because the reaction is driven to a neutral pH. Puck #116's should also react fast and then fall off relatively fast because of the additional acid in the puck. Each puck was placed in the bottom of the reactor. The water was added within the first 30 seconds of the test. No more water was added after that time.

The test is to determine how the $AlCl_3$ effects the overall reaction rate in the pucks. Ideally the reaction should be quick and then stop. The reaction rate of the three pucks are indicated in Figure 11.

Figure 11 shows a clear difference between puck # 113 and pucks #114 & #116 . Puck #113's reaction seems to start off at the same pace as the other two pucks. The reaction peaks early and then drops off quickly. The reason that the reaction peaks early is because the pH in the reactor climbed to around 9-11 which in turn slows the reaction. The pH was taken after the test was over.

Puck #114 was made with the stoichiometric amounts of $AlCl_3$. Initially the puck reacts quickly using the lower pH to drive the reaction. The reaction then peaks and slowly drops off. The reason the reaction is not able to maintain its high rate is the change in pH. If more than the stoichiometric amount of water was added to the reactor over a period of time, then the reaction would have run longer at a faster rate. The reactants composition drives the reaction to a neutral pH. In the plane of the puck the pH changes from the centerline to the edge. This yields several different reaction rates within the puck. The pH in the structure is then hard to control. This could be a problem when trying to shut the system off because of the continued reactions.

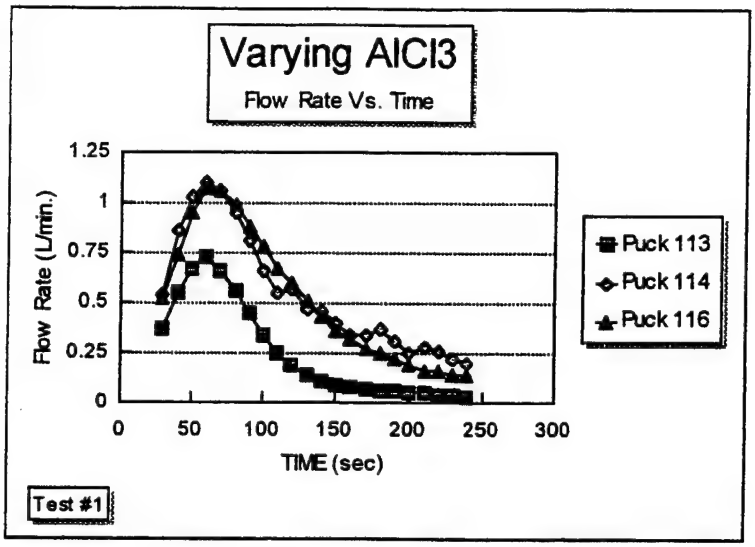

Figure 11

Puck #116 has 1.5 times the stoichiometric amount of $AlCl_3$, so it should react fast and quickly drop off. As seen in Figure 11 the puck operation was similar to puck #115. The only difference between the two is that after #116 peaks the drop in H_2 evolution is slightly steeper. This means the reaction starts off quickly and then falls off slightly faster than puck #114. Theoretically this reaction should be ideal. The reaction has enough acid to go to completion. The problem is the ratio of $AlCl_3$ to $NaBH_4$ is too high. The water has trouble migrating through the thick reactants. Puck #116 had a thickness of 0.400" which is 25% thicker then puck #114 . This means the flow path for the water is extended between $NaBH_4$ particles.

Test 2

The purpose of this test is to determine the effect thickness has on the puck performance. The test is based on findings from test one. The test uses pucks with the high $AlCl_3$ levels to see if it will quicken their overall reaction rates. Two pucks were made each having equal percentages of reactants. The two pucks differ only in thickness.

Puck #116 was used from the last test. Its thickness is 0.400"

Puck # 117 is made with : 2.5 grams $NaBH_4$
8 grams of $AlCl_3$*6 H_2O
2.5 grams of epoxy
Thickness = 0.200"

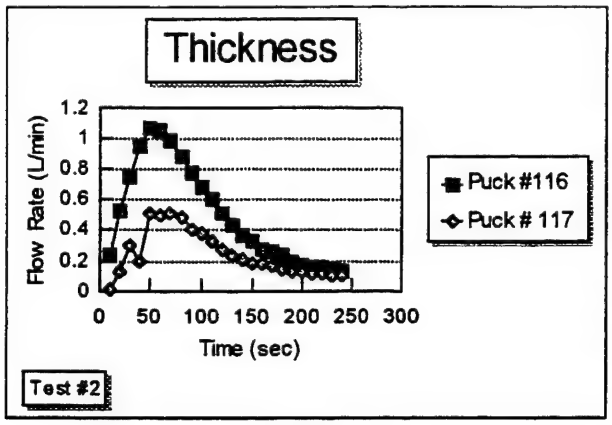

Figure 12

The test shows the reaction rate of puck #117 is approximately half the rate of puck #116. This shows there is not a direct relationship between reaction rate and puck thickness. We were hoping to see a fast initial reaction greater than or equal to the larger pucks and a fast decline. The reaction rate seems to be related to the amount of $NaBH_4$ available in the puck. The high $AlCl_3$ content in the puck should run the reaction faster regardless of its thickness. Puck #117 being half the size and thickness not being a factor, one would expect the puck to yield half the hydrogen at the same rate. Puck #117 liberated hydrogen at half the rate of the thicker puck. The difference between the two pucks is their thickness. They hold equal ratios of reactants. The change in surface area is only 14% between the two pucks. The larger puck had twice the $NaBH_4$ for approximately the same surface area. This may account for the increased performance with the thicker puck. The total surface area of reactant inside the puck is more important than the geometric surface area of the puck. The results show that the loss of "internal surface area" due to products generation causes the reaction rate to fall. The hydrogen evolution rate is mass transport limited.

Test 3

In test 3 a thick puck was made with stoichiometric amounts of reactants. This puck was then placed in the reactor with 5 times the water needed to go to completion. The puck should have liberated 18 liters of hydrogen. This test objective is to determine if the epoxy is encapsulating any reactants. The puck used $NaBH_4$, $AlCl_3*6H_2O$, and epoxy(DP-110) and was pressed at standard conditions of 750 psi contact pressure for 15 minutes at room temperature. The test showed that the water transport through the puck is poor. The yield was only half of the theoretical yield. The puck was then placed in the oven and dried for 30 minutes. After the puck was dried it was cut open for inspection. It was found that the center wasn't reacted. The thickness of the puck in this case was important. The volume of the puck had increased approximately 10 % with no hydrates forming externally. The increased volume may be attributed to the water in the puck. The water when driven off through drying leaves behind the hydrates that formed inside the puck rather than on the pucks surface. The water transport problems are linked to the pore size inside the puck.

PUCK CHARACTERISTICS

	Puck #114		**Puck #116**
Size	0.24 in. thick 2 in. wide 2 in. long	Size	0.40 in. thick 2 in. wide 2 in. long
Volume	0.96 in^3 5 grams $NaBH_4$ 5.2 grams/in^3	Volume	1.6 in^3 5 grams $NaBH_4$ 3.125 Grams/in^3

The three tests have given us a better understanding of the reactant materials. The most important issues are in the area of water management. The introduction of water to the system may be the

most difficult aspect of the system The data shows that the thickness, surface area and pore size of the puck can contribute to its overall performance. In isolating the thickness, we determined that its relative to the materials being used.
The first tests focused on two pucks. Puck #114 had the stoichiometric amounts of each reactant. Puck #116 had 1.5 times the stoichiometric amount of $AlCl_3$. Puck #114 and puck #116 each had equal amounts of $NaBH_4$ and an equal percentage of epoxy.

Figure 13 illustrates the penetration depth of the water into the pucks. This shows the depth vs. hydrogen flow rate of the pucks. The only difference in the two performance lines is the depth of penetration. Puck #114 has a hydrogen evolution rate of approximately 1.10 L/min. at a depth of 0.012 inches into the puck surface. The volume of puck being used at 0.012 inch is 0.048 in^3. This correlates to approximately 0.25 grams of $NaBH_4$. The hydrogen evolution slowed to a minimum at a penetration depth of around 0.058 inches. The total puck volume which was used is 0.232 in^3 which means 1.20 grams of $NaBH_4$ was used in the reaction.

Puck #116 has a hydrogen evolution rate of approximately 1.10 L/min. at a depth of 0.020 inches into the puck. The penetration depth is 40% deeper than puck #114 at the same rate. The volume of the used portion at 0.020 inches depth is 0.080 in^3. The amount of $NaBH_4$ in that portion is approximately 0.25 grams. The two pucks had the same evolution rates at different depths over the same time period. They also utilized the same quantity of $NaBH_4$ at the maximum evolution rate. Puck #116's overall penetration depth was approximately 0.070 inches which is 17% deeper than puck #114. The difference between the two pucks is the additional $AlCl_3$ in puck #116 which adds thickness. The $AlCl_3$ also keeps the pH lower so the reaction will be sustained. The reaction still slows down short of completion, leaving much of the reactants untouched. The ideal thickness is dependent on the materials being used. The thickness for puck #114 should be 0.010 to 0.015 inches thick for the reaction to remain steady. The thickness for puck #116 should be 0.019 to 0.025 inches thick.

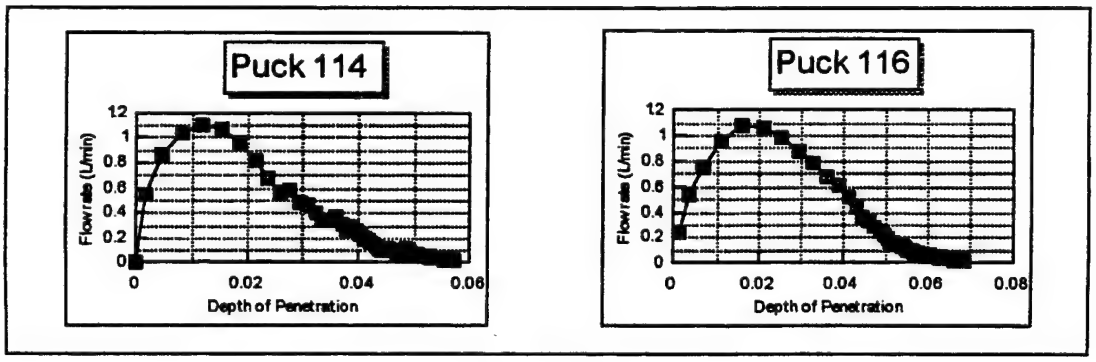

Figure 13

Manufacturing a thin puck is very difficult. The epoxy composite must have a very fine particle size. The problem with die casting epoxy composites is distributing the fine powder in the die uniformly. The percentage of epoxy within the composite is also a critical factor.

Test 4

The next step was to investigate materials which may have a thicker cross section. The test will show the structural integrity of the test pieces through visual inspection. The percentage of binder in the pucks can effect it in two ways. One way is by shielding the reactants from the water. The other way is if there isn't enough binder the puck falls apart before the water is able to wick to other reactants. The tests were performed using $NaBH_4$, $CoCl_2$ and epoxy. The amount of $CoCl_2$ is surprisingly small compared to the other compounds we have tried. This is because only $1/45^{th}$ of the stoichiometric amount is needed to drive the reaction to completion. The cobalt acts as a catalyst which drives the reaction. A group of five pucks were made each having equal amounts of reactants.

Puck's # 119 through 123 each had 80% $NaBH_4$, 7.5% $CoCl_2$, and 12.5% epoxy(DP-110). They were stacked together and held upright in the reactor. Water was admitted into the reactor at a flow rate of about 0.82 ml/min. The stoichiometric amount of water for this reaction was approximately 50 ml . The test duration was 60 minutes. Liquid water was admitted directly onto the top surface of the pucks. A hole in the reactor bed formed where the pucks reacted. The hole was 1 inch in diameter and was as deep as the length of the puck. The remaining reactants were untouched. The low percentage of epoxy in these pucks was insufficient to maintain their structural integrity. When the puck structure is altered it loses its wicking capabilities and water is no longer distributed to active sites.

3.4.5 Fabrication Research

Tests were done on various types of binders. The tests where directed towards changing the binder percentages to see how the structure is affected. Tests using low epoxy content (12%-20%) were easy to handle and fabricate. These mixtures resemble cake crumbs. The higher epoxy percent mixtures exhibited mold release problems and were hard to handle. The mixture agglomerates forming a non homogeneous structure when pressed. The weight/reactant ratio also suffers at increased binder content.

In most plastics a filler is added to increase its strength. Talc, fiberglass, graphite and kevlar are fillers that are often used. In the structure that we prepared the two powders are a poor filler choice. The fiber glass and the kevlar could be used because of their fibrous nature. The fiberglass may cause some problems because of its high calcium content. The calcium could poison the fuel cell. Tests were performed using kevlar pulp as a filler to strengthen the puck structure. The kevlar pulp was blended to break down the fiber particle size. It was then added to the mixture of puck reactants and epoxy. Several different percentages were tested in order to optimize the pucks structural integrity. The blend of reactant and binders with the best results were:

60 % $NaBH_4$
4.0% $CoCl_2$
26% Epoxy (dp-420)
10% Kevlar pulp
Pressed at 500 psi contact for 20 min., left overnight.

The structure was retained in water but the reaction rate slowed considerably. This could be due to the high levels of epoxy. Kevlar pulp by itself is hydrophilic and may act as a wick in the

structure. The epoxy in the structure may absorb into the kevlar preventing wicking.. A rigid filler such as fiberglass may have a better chance of holding the puck together with limited absorption of the epoxy.

Tests were performed on several different adhesives binders from silicone potting compounds to petroleum jelly.

3.4.5.1 Silicone Potting Compound

Curing time is heat dependent, 15 minutes at 125 degrees C. The work life at 25 degrees C is 24 hours. The silicone potting compound is easy to work with because the mixture remains soft and moldable. The silicone isn't a hard substance so the end result is not a rigid matrix. The puck seemed to be hydrophobic because of the silicone, but cutting into the puck improved water accessibility to the reactants. Changing the percentage of the binder may improve the wetting properties but it will also weaken the structure.

3.4.5.2 Urethane Casting Resin:

Curing time/pot life is 20 minutes at 25 degrees C, fully cured in 16 hours. The urethane resin has a high strength but a low heat distortion temperature of 110 °F. The pucks normally run at 120 to 200 °F locally. The urethane resin breaks apart at those temperatures. The resin also seems to react slightly with the other puck ingredients giving it a slight discoloration.

3.4.5.3 Kynar Powder (Polyvinylidenedifluoride)

This is a very fine powder with a melting point of around 350 °F . This powder was mixed with the reactants and placed in a die. The die was then put under pressure and placed in the oven at 360 °F. for 20 minutes. The product was a ceramic like wafer that is very brittle and buoyant. This powder is very easy to work with and the work life is indefinite. The only way to cure this binder is by heating. The fine powder settles to the bottom of the puck. The pucks wicking capacity seems to be very poor, since it floats.

3.4.5.4 Petroleum Jelly

A mixture of $NaBH_4$ and $CoCl_2$ was mixed in with a percentage of white petroleum jelly, to see if it would react. The slurry seemed to be stable. This combination wouldn't be acceptable for making a puck, because it would never cure. The idea of making a paste is one that hasn't been explored. Petroleum jelly is very hydrophobic so using water wouldn't work in the reactor. Replacing the water with an acid that eats through the petroleum jelly and react with the $NaBH_4$ can work. This process would eliminate the use of $CoCl_2$. The problem with petroleum jelly is that it leaves an oily film on top of the acid which may inhibit the transfer of acid to the $NaBH_4$. The percentage of petroleum jelly needed may result in a poor mixture and a heavy, unworkable paste.

The investigation of a stable matrix for a puck has not been determined. The research shows that the system can dictate the configuration of the reactants. Research on microstructures, porosity, and wicking would clarify the problems with pucks. The water transport problems in the puck matrix has pushed us to using the cobalt chloride doped pellets. These pellets are approximately 5/16 " in diameter and liberate 500 ml. of H2 each when water is supplied. The pellets are easy to

handle and are readily available. The problem with these pellets are the large quantity of hydrates that form during the reaction.

3.4.5.5 Acid-$NaBH_4$ Reactor

The use of an acid with the $NaBH_4$ is another option which we have investigated. In theory, if an acid is added to $NaBH_4$ it will react very quickly. For safety reasons the acid should be weak. The system we looked at uses acetic acid and $NaBH_4$ pellets.

$$NaBH_4 + 3\ H_20 + CH_3CO_2H \rightarrow B(OH)_3 + 4\ H_2 + NaC_2H_3O_2$$

The reaction looks promising but yields a heat release of -284 Kcal/mol. which is much too high. The other problem is that 1 mole of acetic acid is required for every 3 moles of water. The solutions normality was around 18 N. which is very concentrated. The product residue was similar to a wax paste and didn't seem water soluble.

3.4.6 Reactor Configuration

Investigating different configurations for a generator we have set certain parameters to follow. The first criterion is for the reactor to be light weight and have a low volume. The weight and volume must be competitive with bottled hydrogen. The second criterion requires that the reactor be position insensitive. The third criterion faces the issue of weather conditions. The operating temperatures for the reactor should be between 0 and 100 degrees F.

3.4.6.1 Binary Liquid Generator

The binary liquid generator mixes two liquids to generate hydrogen. One liquid is $NaBH_4$ and water in a basic medium. The solubility of $NaBH_4$ in water is approximately 0.3 grams of $NaBH_4$ in 1 ml of water. The second liquid is a mild acid 20 normal H_3PO_4. The idea behind the binary liquid generator is that two liquids mix quicker and more uniformly than a liquid and a solid. This making it easier to control. There are two components in the reactor configuration. The reactor compartment holding the H_3PO_4 and the other holding the liquid $NaBH_4$. The $NaBH_4$ is metered into the acid compartment at a rate which produces the desired amount of hydrogen. The control system uses a pressure switch to control a solenoid valve between the two liquid compartments. The $NaBH_4$ liquid is add to the acid through the solenoid when the reactor pressure is low. This increases the pressure in the reactor and turns the pressure switch off, stopping flow.

The binary liquid generator works perfectly within some constraints. The problem with this system is the added water that is needed to dissolve the $NaBH_4$ adds weight and volume to the system. Another problem is that the $NaBH_4$ precipitates at 40° - 50 ° F and starts to react at higher temperatures. This makes the system difficult to control. In ideal conditions this is a reasonable hydrogen generator, but because of the solution instability it didn't meet our criteria.

3.4.6.2 Bar Generator

The Borohydride Anode Recycle approach uses the water from the anode side of the fuel cell to drive the generator. The generator uses a packed bed of $NaBH_4$ pucks to capture the water from the humidified hydrogen stream. The water captured by the $NaBH_4$ reacts and produces more hydrogen and water. This is a closed system and needs a pump to keep a continuous flow of hydrogen. The research performed on pucks was to be integrated for this system. The fuel cell would have to be modified to recapture cathode water for this system to work. The modifications

to the fuel cell stacks would be to alter the reactant gas flow. The resulting, dry cathode exhaust could yield cell performance problems.

3.4.6.3 LSB Generator

The Liquid Solid Borohydride generator uses solid $NaBH_4$ and a catalyst with liquid water. The configuration of the $NaBH_4$, its catalyst, and the binder are very important. Since we have determined that the thickness vs. reaction rate of pucks causes the overall yield to decrease , we decided to use the $NaBH_4$ * $CoCl_2$ pellets which can be purchased commercially. The LSB generator uses two separate containers. One holding the solid $NaBH_4$ * $CoCl_2$ pellets the other holds the water. The water is forced into the reactant container and reacts with the NaBH4. This type of reactor needs a control system that measures pressure and uses a time circuit for the water input.

3.4.6.4 Design (LSB Generator)

The LSB design uses a slightly pressurized vessel with two compartments. The two compartments are separated by a partition which threads into the top and bottom compartments. The top is the reactor chamber and the bottom is the water chamber. A solenoid valve, located in the top compartment, separates the water and the reactants. The solenoid is controlled by a timing circuit and a pressure switch. The reactants are encapsulated in a hydrophobic container so the reactants never come in contact with the reactors walls. The reactant container also makes it easy for recharging the generator by just replacing it.

Several tests were performed on water inlet control, and on containing excess H_2 after shut down. A control system has been designed to inject a given amount of water then wait for pressure to build. A pressure switch turns the solenoid on and off at the specified pressures.

The reactor is made of 6061 aluminum alloy and has a anodized finish. The problem working with pressurized systems is the container. The initial design called for a pressure of 500 psi (max) because of the size constraints. The problem was finding a small light weight regulator for that pressure range. The small regulators are limited to 300 psi. This defined the allowable pressure range. The pressure is dictated by the lag time between turning off the water supply and the time it takes for the water react. The average time for the hydrogen evolution to slow down is between 9 and 15 minutes. The hydrogen volume for a reaction of 15 minutes at 2 liters a minute is approximately 1.05 ft^3 of hydrogen. A excess volume in the top compartments is set aside for this added volume of hydrogen. The compartment is also designed to handle the additional pressure of 300 psi.

The system also uses a pressure relief valve in case of over pressurization. Regulators and a filter are added to the reactor . The added weight of these components make the total weight of the system approximately 6.5 lbs.

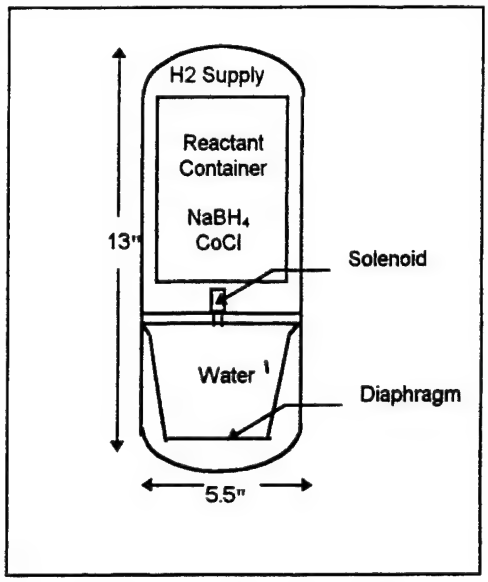

REACTOR SPECIFICATIONS
750 WATT HOUR MISSION

Total H_2	=	0.0441 lb Mol.
Total $NaBH_4$	=	448 lbs.
Total H_20	=	30 lbs.
Reactants Total Weight	=	1.25 lbs.
Reactor Shell Volume	=	200 in^3
Reactor Shell Weight	=	4 lbs.
Reactant Container Volume	=	37.1 in^3
Water Diaphragm Volume	=	0.37 liters

Pressurization the bottom container is used as the mechanism for adding the water into the reactor. The bottom container holds a diaphragm which is filled with water. The water is forced into the top container through a solenoid using a pressurized gas on the back side of the diaphragm. The gas is admitted through a one way valve at the bottom of the container. The reason we are using gas pressure is because of the size constraints. Most alternatives increase the size substantially. The delivery pressure needed must be higher than the low pressure limit of the reactor. The delivery pressure will than change through the course of the reaction, due to reactant/product volume changes.

Tests were performed on a similar system using the timing circuit and the solenoid to determine how the they will work together. The timing circuit is set up for a 50% duty cycle.

Figure 14 illustrates the pressure and flow rate as a function of time. The flow rate shows several 5 SLPM spikes. These spikes occur when water is admitted into the reactor. The pressure in the vessel stays constant because of a back pressure regulator. During the test the flow was stopped to let the reactor build pressure. The initial pressure increase was a test to see the high pressure limit for the amount of water introduced. The maximum pressure that this test had recorded was 50 psi. The test vessel used has a slightly smaller volume than the reactor unit designed for this application.

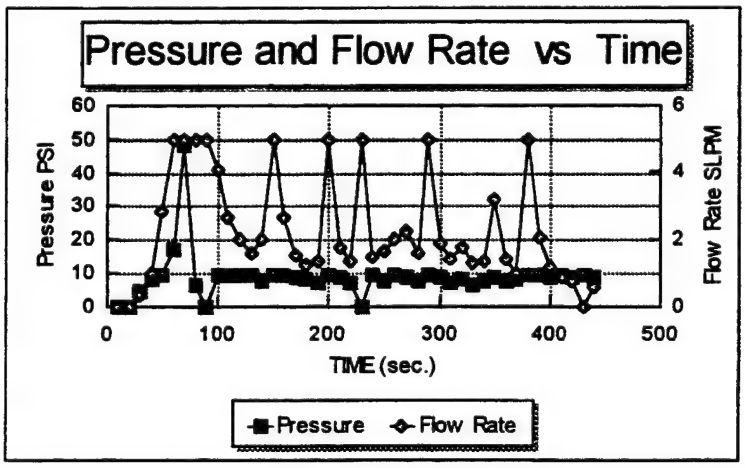

Figure 14

The initial reactor was to run continually at 2 liters/min. until it was shut down. The tests for a reactor to accomplish that showed a lag time between shut down and hydrogen production stoppage. This lag time gave us an unwanted hydrogen volume which increased the total volume

of the reactor. The idea that different reactant combinations of configuration would make any difference on the lag time has been explored. The water transport problems with the pucks are due to the structure and what is made in the reaction. The reaction makes hydrates which makes water transport difficult. The hydrates are something that we can only control with excess water. The reactor that has been designed is just a control system that doesn't worry about the reactants and what they make. In the future more work should be done on perfecting a better control system. The reactor could be made smaller and lighter depending on the accuracy of the control system.

3.5 Manufacturing Technology

3.5.1 Performance Endurance (P/E) Test Rig Design & Construction

During this program a test rig was designed and built.

3.5.1.1 Test Rig Design

The purpose of the P/E test rig is to determine the effect of load variation and operating

Table 3

Stack Test Matrix

Independent	Dependent
Relative Humidity	Resistivity
Pressure	Voltage
Mass Flow (% Utilization)	Current
Test Time	Cell Temperature
Load on stack	

conditions on fuel cell performance. Table 3 is the stack test matrix which was executed during rig testing is listed below.

The P/E test rig has four stations. The capability of each station is shown in Table 4. The numbers listed to the right of the gas specifications are the maximum station flow rates in SCFM.

Station 1 is a 10 cell 64 watt sub-stack test station with air via free convection. This station records relative humidity, anode pressure, stack temperature, voltage, current and resistance. Station 4 is the same as Station 1 except that the load bank is designed to handle 250 watts.

Table 4

P/E Test Rig Station Specifications (Original Design)

STATION #	STACK SIZE	H_2 MANIFOLD	AIR & O_2 MANIFOLD
1	64 Watts	.03 SCFM	-
2	64 Watts	.03 SCFM	0.27 SCFM
3	64 Watts	.03 SCFM	3.53 SCFM
4	250 Watts	.11 SCFM	-

Station 2 is a 10 cell sub-stack test station with air and oxygen manifolding to allow forced flow through the cathode. Forced flow is measured through the cathode with utilizations down to 25% (.27 SCFM). Station 3 is the same as Station 2 except that the air/oxygen utilization can drop to 2% (3.53 SCFM).

For all stations, the design pressure is 60 psia and the design temperature is 140 °F. The saturators in each test station hold about 2.7 L (.7 gal) of water. This is sufficient to saturate air flowing at .27 SCFM and 140 °F for 35 hours of continuous operation.

3.5.1.1.1 Saturator Design

The saturators were designed to provide saturated gases to either side of a 250 watt fuel cell stack for an extended period of time. The saturator body consists of a 4" I.D. cylindrical tube 16" long. The tube is closed at one end with a flange welded to the opposite end. A cap sits on top of the flange. This cap provides a sealing surface for the flange O-ring and a gas port.

A flange is welded to the top of the saturator. The flange O-ring in combination with six 1/4" bolts provides sealing under internal pressures of greater than 100 psia (to ASME code). The cap also allows for manual water refill and temperature measurement through NPT.

The incoming gas is saturated as it passes through a low-pressure drop porous sparger. Once through the sparger, the gas rises to the surface and becomes saturated. It exits the saturator through the cap and proceeds to the cell stack. A light on the rig panel is activated when the water level in the stack drops below the level sensor. The saturator is heated with a 1" wide tape heater fastened its base. The 500 watt heater brings the saturator to 140 °F in 15 minutes. A temperature controller is used to keep the water in the saturator at the desired temperature. The bolted top construction of this saturator allows for ease of disassembly.

3.5.1.2 P/E Test Rig Status

3.5.1.2.1 Structure

The P/E test rig is constructed from Unistrut and Plexiglas. It is divided into two sections. One section contains Stations 1 and 2; the other Stations 3 and 4. Each section is approximately 5' long by 2' wide by 2' high allowing ample space for the saturators and the external manifolds on the air side of each station. The instrumentation and electronics are mounted on the front and side Plexiglas panels.

3.5.1.2.2 Instrumentation

The instrumentation consists of pressure gauges, RTD's, thermocouples, rotameters, electronic mass flow meters, and relative humidity sensors. The RTD's are used to measure the saturator temperature and this signal is fed back into a temperature controller. The thermocouple is used to monitor stack center-line temperature. An AD594 will be used in combination with the thermocouple to provide a 0 to +5 volt output that is linear with stack temperature. The relative humidity sensors are mounted in a stainless pipe that can be connected to 1/4" tubing via NPT fittings. These sensors can monitor relative humidity from 30-100% over a temperature range of 70-150°F.

3.5.1.2.3 Plumbing

Quarter inch 304 SS tubing is used to join the metering valves, shut off valves and check valves. The metering valves were sized so that the Cv of the valve is obtained at about 75% of the maximum flow that it sees. The shut off valves and check valves are standard. The check valves have a cracking pressure of 2 psi, which is adequate for our purpose.

3.5.1.2.4 Electronics

The signals provided by the instrumentation are collected and amplified. Table 5 identifies the 15 output signals for Section made up of Station 1 and Station 2 To handle the 30 signals for the P/E Test Rig, we purchased 2 A/D boards, each with 16 channel capability. The two spare channels can be used for intermittent measurement of the line temperature downstream from the saturators.

Table 5

STATION 1	STATION 2
Relative Humidity (H_2)	Relative Humidity (H_2,O_2)
Pressure (H_2)	Pressure (H_2,O_2)
Voltage	Mass Flow Rate
Current	Voltage
Resistance	Current
Stack Temperature	Resistance
	Stack Temperature

3.5.1.3 Upgrades

During the program the P/E test cell rig was modified in order to test high power and high flow rate stacks. Stations 1-3 were originally designed to test 10 cell sub-stacks. Station 1 remains a substack testing unit. Stations 2 and 3 were upgraded to handle higher hydrogen and air flow rates. Station 2 runs the FC-150 and station 3 or 4 can run the FC-200. Station 4 remains a fan testing unit. By eliminating the fan and connecting the air side of a stack directly to the rig we can measure its exact flow requirements. A ducting systems at the stack air side inlet provides uniform flow across the inlets and accurately measures pressure drop.

An electronic load allows us to test stacks in either constant current or resistance modes. The load can handle currents up to 150 amps and a total power of 750 watts. It has two stations and is capable of running two stack simultaneously or one large stack when connected in series. The load allows us to run any size fuel cell stack and produces a smooth performance curve from open circuit to short.

3.5.2 Process Development

3.5.2.1 Cell Fabrication

The cell fabrication process consists of several steps. The first step requires mixing a batch of catalyst ink. The recipe consists of a 5% Nafion solution in alcohol, and 40% Pt on Vulcan XC-72 catalyst from E-Tek. Additional solvents can be used to adjust the ink viscosity such as isopropanol. The ink is screen printed onto both sides of a piece of DuPont Nafion NX-112F membrane. Several printings are required to obtain the correct catalyst loading of 0.5 mgm/cm^2 of

active area. After printing is complete, the cells are pressed at 300 psi pressure and 260°F for 2 minutes.

The printed cells are treated in a hydrolysis bath. The hydrolysis solution converts the membrane from the sulfonyl fluoride form to the potassium form. The membranes are rinsed in water and then placed into two separate nitric acid baths for approximately 30 minutes. This completes the conversion of the membrane to the proton form.

After chemical processing the cells are air dried flat, die cut and checked in the single cell test fixture. This fixture, which was developed under the Phase II program is used to detect gas crossover and ensure that each cell is pinhole free before being placed in a stack.

In the following section we will discuss some of the cell fabrication problems we have encountered.

3.5.2.1.1 Hydrolysis

The hydrolysis step is the most time consuming of the cell fabrication process. It takes several hours and requires constant temperature and agitation of the chemical baths. Analytic Power set up a hydrolysis facility in its fuel cell factory to increase the speed of cell fabrication.

The role of the solvent in the bath is to swell the membrane so the sulfonyl fluoride can be hydrolyzed to potassium sulfonate. Our 25 watt cells measuring 2.5" x 2.5" active area are processed in the hydrolysis facility without any difficulty. Larger ARO cells, however, were found to cross over after drying. We traced the problem to several sources. The primary source of pinholes are gels present in the original membrane. If the catalyzed membrane is pressed in a platen press, these pinholes act as stress concentrations and will be pinholes after the membrane is hydrolized. In general, the presence of a catalyst layer on the membrane slows the hydrolysis process because the solution has to diffuse through the catalyst layer first.

The 250 watt cells have an active area of 7.3" x 2.6" and hang in the bath the long way (to a depth of about 7.5"). Wet cells show no evidence of crossover in our test hardware but they crossover when dry. To prove that the depth made a difference we processed two identical 250 watt cells and hung them perpendicular to each other. Both cells sealed when wet but the cell processed deep in the bath crossed over when dry. The cell processed in the top portion of the bath sealed when dry. A further problem we encountered was that alcohol vapor was igniting in the presence of the catalyst while dipping the cells into the tank.

In the past we used titration as a method of determining whether hydrolysis was complete. We have since found that the thickness of the membrane may vary by 20% and the ion exchange capacity varies with it. This limits the value of titration as a tool to determine the conversion of membrane from the sulfonyl fluoride to proton form.

3.5.2.1.2 Printing And Catalysis

3.5.2.1.2.1 Transfer Catalyzation

To speed production time we tried to transfer catalyze a membrane rather than directly print onto the membrane. One cell was screen printed onto Nafion backing paper rather than on the membrane directly since membrane handling is difficult and time consuming. The membrane sticks to itself and must be taped to a surface during screen printing. Further, when lifting the membrane from the surface to print the reverse side, catalyst particles often pop off of the membrane. Also careful registry of the membrane is required to ensure that the active area is aligned on either side.

The advantage of transfer catalyzation would be ease of setup in the screen printing machine as well as decreased fabrication time. Many electrodes could be printed at a time without having to register them or handle the membrane. Once printed the catalyst layers are sandwiched around the membrane and steam pressed onto it. Unfortunately, along with the catalyst layer, some paper ingredients are also transferred. The resulting cells performance was fair. This method could still be used if we can identify a surface other than standard papers on which to print the catalyst.

3.5.2.1.2.2 Screen Printing

To effectively utilize the screen printing machine for printing cells we need to eliminate alcohol from the mixture. As the alcohol evaporates, the ink dries and clogs the screen mesh. This requires frequent cleaning of the screen which not only wastes ink but also time. Our normal ink is made with a 5% Nafion/alcohol solution.

We made ink mixtures using Nafion solution with alcohol in place of by other solvents. These cells did not perform as well as those made with alcohol. Work performed in another program showed that the Nafion in the ink can stratify and that drying the catalyst layer between printings is a very important step.

3.5.2.1.2.3 Catalyst Ink

In order to streamline the cell printing process, we need to eliminate isopropanol from the catalyst ink mixture. In so doing we could prevent alcohol evaporation from changing the ink consistency. Isopropanol has a low equilibrium vapor pressure and readily evaporates at room temperature. The results are twofold. Changing the ink viscosity results in non-uniform catalyst loading from cell to cell. Evaporation also causes the ink to dry within the screen pores which interferes with subsequent screen printing.

The source of the isopropanol is the 5% Nafion solution we use. The alcohol in the mixture digests the Nafion and maintains it in a liquid state thereby ensuring a homogeneous solution. By replacing the isopropanol with a higher vapor pressure alcohol the catalyst ink will maintain its consistency. Storage of the ink is an important factor. It must be stored in a glass container since plastic is permeable to oxygen which can react with solvent components.

3.5.2.2 Grooving Machine

We had planned to purchase a grooving machine since our carbon paper suppliers were reluctant to provide pre-grooved substrate at a reasonable cost. Our anode frame design requires accurate groove alignment. After a lengthy search it became obvious that we would not be able to buy one within our budget - most used machines we looked at cost well over $10,000.To resolve this problem we designed and built a grooving machine. The major components include, positioners, carbide cutting wheels, motor, and linkages. It is essentially a scaled version of a horizontal milling machine with a foot print of 36" X 24".

The manual Y-axis positioner mounted on a motorized X-axis is used to adjust and feed the carbon flow field under the carbide saw blades. Groove depth on the carbon flow fields can be varied by adjusting the height of the saw gang arbor via the manual Z-axis positioner.

A water spray is applied to the cutting wheels and grooving target to rinse away the dust and debris. Grooving a wet piece of carbon eliminates any free floating dust from the air. The carbon sludge is washed into a tank and collected in filtration bags to keep the water circulation clean.

3.5.3 Reactor Test Stand

The test stand is designed for running solid and liquid chemical hydride hydrogen sources. The components are rated to approximately 1500 psi (max.) and are chemically stable. The flow requirement is 0-2.5 liters per minute of hydrogen. Two flow measuring devices have been installed on the test stand. The first is a mass flow meter which is used for collecting data. The second device, a rotameter mounted on the front panel, is used for a manual check.

The test stand is equipped with two cooling systems. One for cooling the hydrogen as it comes out of the reactor. The second for cooling the reactors casing to slow down the reaction rates. In addition to the cooling system there is a reactor heater which is used for controlling reaction rates.

The reactor is made of a 304 stainless steel nipple with two 3000 psi threaded end caps. The top end cap has four holes drilled and tapped for gas exits and reactant inlets. There is a thermocouple through plug that will allow four thermocouples to be placed inside the reactor for temperature distribution testing. The test stand includes two pumps, two fans, six thermocouples, a pressure transducer, mass flow meter and band heater. A die was designed for molding the $NaBH_4$ powder mixtures into 2" x 2" corrugated pucks.

4. REFERENCES

"Heat Removal in Ambient Pressure PEM Cell Stacks," V. Bloomfield, J. Kelland, P. Grosjean, D. Bloomfield, Proceedings of the 36th Power Sources Conference, 6-9 June, 1994

"Century Series Power Supplies," D. Bloomfield, 1994 Fuel Cell Seminar, Nov. 28-Dec. 1, 1994.

C062AR01 1 January 1993 - 31 December 1993
Progress Report

C062TR01 No Date
SBIR Phase II Mobile Electric Power
Interim Technical Report

C062TR02 No Date
SBIR Phase II Mobile Electric Power
Semi-Annual Technical Report

C062TR03 Date March 14, 1995
Interim Technical Report

C062TR04 14-Mar-95
Interim Technical Report

C062TR06 03/14/95
Interim Technical Report

C062TR07 9/1/94
Interim Technical

C062TR08 10/11/94
Interim Technical Report

C062TR09 3/14/95
Interim Technical Report

5. SCIENTIFIC PERSONNEL INVOLVED

David Bloomfield
Valerie Bloomfield
Paul Grosjean
James Kelland